

This article was downloaded by: [93.150.144.95]

On: 19 June 2015, At: 06:43

Publisher: Taylor & Francis

Informa Ltd Registered in England and Wales Registered Number: 1072954 Registered office: Mortimer House, 37-41 Mortimer Street, London W1T 3JH, UK



## Journal of Difference Equations and Applications

Publication details, including instructions for authors and subscription information:

<http://www.tandfonline.com/loi/gdea20>

### Border collision and fold bifurcations in a family of one-dimensional discontinuous piecewise smooth maps: divergence and bounded dynamics

Roya Makrooni<sup>a</sup>, Farhad Khellat<sup>a</sup> & Laura Gardini<sup>b</sup>

<sup>a</sup> Faculty of Mathematical Sciences, Shahid Beheshti University, Tehran, Iran

<sup>b</sup> DESP University of Urbino Carlo Bo, Urbino, Italy

Published online: 19 Jun 2015.



CrossMark

[Click for updates](#)

To cite this article: Roya Makrooni, Farhad Khellat & Laura Gardini (2015): Border collision and fold bifurcations in a family of one-dimensional discontinuous piecewise smooth maps: divergence and bounded dynamics, *Journal of Difference Equations and Applications*, DOI: [10.1080/10236198.2015.1046855](https://doi.org/10.1080/10236198.2015.1046855)

To link to this article: <http://dx.doi.org/10.1080/10236198.2015.1046855>

PLEASE SCROLL DOWN FOR ARTICLE

Taylor & Francis makes every effort to ensure the accuracy of all the information (the "Content") contained in the publications on our platform. However, Taylor & Francis, our agents, and our licensors make no representations or warranties whatsoever as to the accuracy, completeness, or suitability for any purpose of the Content. Any opinions and views expressed in this publication are the opinions and views of the authors, and are not the views of or endorsed by Taylor & Francis. The accuracy of the Content should not be relied upon and should be independently verified with primary sources of information. Taylor and Francis shall not be liable for any losses, actions, claims, proceedings, demands, costs, expenses, damages, and other liabilities whatsoever or howsoever caused arising directly or indirectly in connection with, in relation to or arising out of the use of the Content.

This article may be used for research, teaching, and private study purposes. Any substantial or systematic reproduction, redistribution, reselling, loan, sub-licensing, systematic supply, or distribution in any form to anyone is expressly forbidden. Terms &

Conditions of access and use can be found at <http://www.tandfonline.com/page/terms-and-conditions>

## Border collision and fold bifurcations in a family of one-dimensional discontinuous piecewise smooth maps: divergence and bounded dynamics

Roya Makrooni<sup>a,1</sup>, Farhad Khellat<sup>a,2</sup> and Laura Gardini<sup>b,\*</sup>

<sup>a</sup>Faculty of Mathematical Sciences, Shahid Beheshti University, Tehran, Iran; <sup>b</sup>DESP University of Urbino Carlo Bo, Urbino, Italy

(Received 21 March 2015; accepted 18 April 2015)

In this work we continue the study of a family of 1D piecewise smooth maps, defined by a linear function and a power function with negative exponent, proposed in engineering studies. The range in which a point on the right side is necessarily mapped to the left side, and chaotic sets can only be unbounded, has been already considered. In this work we are characterizing the remaining ranges, in which more iterations of the right branch are allowed and in which divergent trajectories occur. We prove that in some regions a bounded chaotic repeller always exists, which may be the only non-divergent set, or it may coexist with an attracting cycle. In another range, in which divergence cannot occur, we prove that unbounded chaotic sets always exist. The role of particular codimension-two points is evidenced, associated with fold bifurcations and border collision bifurcations (BCBs), related to cycles having the same symbolic sequences. We prove that they exist related to the border collision of any admissible cycle. We show that each BCB, each fold bifurcation and each homoclinic bifurcation is a limit set of infinite families of other BCBs.

**Keywords:** piecewise smooth maps; border collision bifurcations of repelling cycles; chaotic repellers; codimension-two bifurcation points; unbounded chaotic sets

### 1. Introduction

Piecewise smooth (PWS) systems have been widely investigated in the last decade, due to the large number of non-smooth systems proposed in several applied fields. For example, in physical and engineering systems, a recent survey can be found in [10] (see also [4]). Many applications in engineering may include specific nonlinearities in the map, as power functions. In particular, much attention has been devoted to the square-root singularities in impact oscillators, following the works of Nordmark ([17], [18]). In this paper we consider the PWS map proposed in [13] given by

$$x \mapsto f_{\mu}(x) = \begin{cases} f_L(x) = ax + \mu & \text{if } x \leq 0 \\ f_R(x) = bx^{-\gamma} + \mu & \text{if } x > 0 \end{cases} \quad (1)$$

where  $a$ ,  $b$  and  $\gamma$  are real parameters and  $\mu > 0$ . As recalled in that paper, this PWS system was already considered by many authors, mainly in the continuous case, for  $\gamma < 0$ . In [7] the normal-form mapping of sliding bifurcations is derived, leading to map (1) with  $\gamma = -3/2$ ,  $\gamma = -2$  and  $\gamma = -3$ , related to different cases of sliding bifurcations. The case with  $\gamma = -1/2$  is considered in [3]. Other examples of grazing and sliding

---

\*Corresponding author. Email: [laura.gardini@uniurb.it](mailto:laura.gardini@uniurb.it)

bifurcations with nonlinear leading-order terms occur in power converters and in non-smooth sliding-mode controls ([1],[5],[6]).

In [19] the map in (1) was considered in the discontinuous case with  $\gamma > 0$ , and some remarks for the particular case with  $\gamma = 1/2$  are reported in [20]. This leads to a particular family of maps in which the function  $f_R(x)$  defined on the right side has a vertical asymptote at the discontinuity point  $x = 0$ .

As in [11] and [13] we consider system (1) for positive values of the parameter  $\mu$ , and for any  $\mu > 0$  the transformation  $(x, a, b, \mu) \rightarrow (x/\mu, a, b\mu^{-\gamma-1}, 1)$  leads from (1) to the following map:

$$x \mapsto f(x) = \begin{cases} f_L(x) = ax + 1 & \text{if } x \leq 0 \\ f_R(x) = (b/x^\gamma) + 1 & \text{if } x > 0 \end{cases} \quad (2)$$

The peculiarities of this family in the range related to an *invertible* map have been studied in [14], where interesting bifurcation structures associated with the presence of the vertical asymptote are described, even if, due to invertibility, chaotic sets cannot exist. In [13] we have considered the case of *non-invertible* map  $f(x)$  in a particular range in which the trajectories cannot be divergent:

$$\text{Range AI} : P_1 = \{p = (a, b, \gamma) : 0 < a \leq 1, b \leq -1, \gamma > 0\}$$

proving the properties of codimension-two points associated with fold bifurcations and border collision bifurcations (BCB) related to cycles having the same symbolic sequence. It was also proved that in Range AI only unbounded chaotic sets can exist, which may lead to robust unbounded chaotic attractors (having the properties shown in [12]). In this work, we are considering the remaining ranges for the parameters, classified as follows (as motivated in the next section):

$$\text{Range AII} : P_2 = \{p = (a, b, \gamma) : a > 1, b \leq -1, \gamma > 0\}$$

$$\text{Range BI} : P_3 = \{p = (a, b, \gamma) : 0 < a \leq 1, -1 < b < 0, \gamma > 0\} \quad (3)$$

$$\text{Range BII} : P_4 = \{p = (a, b, \gamma) : a > 1, -1 < b < 0, \gamma > 0\}$$

As it is used in PWS systems of this kind, we study the system's dynamical properties making use of the symbolic notation based on the letters  $L$  and  $R$  corresponding to the two disjoint partitions

$$I_L = (-\infty, 0], \quad I_R = (0, +\infty) \quad (4)$$

To each trajectory we associate its itinerary by using the letter  $L$  when a point belongs to  $I_L$  and  $R$  when a point belongs to  $I_R$ . A cycle is represented by its finite symbolic sequence. For example, a cycle with symbolic sequence  $RL^n$  (corresponding to a basic cycle) has one periodic point on the right partition and  $n$  on the left one. The symbolic sequence can also be associated with the functions which are to be applied in order to obtain a periodic point of the cycle, as fixed point of a proper composition of the two functions defining  $f$ . As an example, to get the periodic point of a cycle  $RL^n$  on the right side we have to solve the equation  $f_L^n \circ f_R(x) = x$ .

Notice that the point  $x = 0$  is associated with bifurcations of two kinds, BCBs, as well as homoclinic bifurcations of cycles. In fact, whenever a cycle has the periodic points which include  $x = 0$  (and thus also  $x = 1$ ), the parameters are said to be at the BCB values

of the cycle, because they are always related to the appearance/disappearance of the cycle. When a preimage of a periodic point (or pre-periodic point) of a cycle merges with 0, then we shall see that the cycle undergoes a homoclinic bifurcation.

The Ranges AII and BII, in which  $a > 1$ , are characterized by the existence of a repelling fixed point in the partition  $I_L$

$$x_L^* = -\frac{1}{a-1} < 0 \tag{5}$$

so that divergent trajectories certainly exist, with immediate basin  $(-\infty, x_L^*)$ . However, for  $x > x_L^*$  the system can have other attractors as well as chaotic sets.

The investigation (still not complete) of the dynamics occurring when a parameter point  $p = (a, b, \gamma)$  belongs to the different ranges in (3) is the object of this paper. The properties of map  $f$  in each different range are proved making use of a suitable first return map, which exists also when the trajectories are mainly divergent. The plan of the work is as follows. In Section 2 some preliminary results are related to the fixed points of our system and divergent trajectories. In Section 3 it is considered the Range AII (which corresponds to Figure 1 to the interval  $S(b) \in (-\pi/2, -\pi/4]$ ). It is shown that the system has divergent trajectories, as  $-\infty$  is always an attractor with a basin of attraction  $B_\infty$  of positive measure. For  $b < -a/(a-1)$  all the points have a divergent trajectory except for a repelling fixed point  $x_L^*$  and its preimage, while for  $-a/(a-1) < b \leq -1$  a chaotic repeller exists which belongs to the frontier of the basin of attraction  $B_\infty$ . This basin may coexist with the basin of an attracting cycle of period  $n \geq 2$ . The Range B with  $-1 < b < 0$  (which corresponds to Figure 1 to the interval  $S(b) \in [-\pi/4, 0)$ ) is considered in Section 4, and the BCBs of basic cycles with symbolic sequences  $LR^n$  for any  $n \geq 1$  are shown to occur. In Subsection 4.1 the Range BI is considered, showing that the system has non-divergent dynamics and persistent unbounded chaotic sets (mainly of zero measure). A peculiar structure of attracting cycles is illustrated. The existing attracting cycles have symbolic sequences different from those existing in Ranges AI and AII, and are related to periodicity regions issuing from organizing centres at codimension-two bifurcation points. All the existing cycles are characterized by repeated iterations also on the  $R$  side. Codimension-two points due to contact points between BCB curves and fold bifurcation

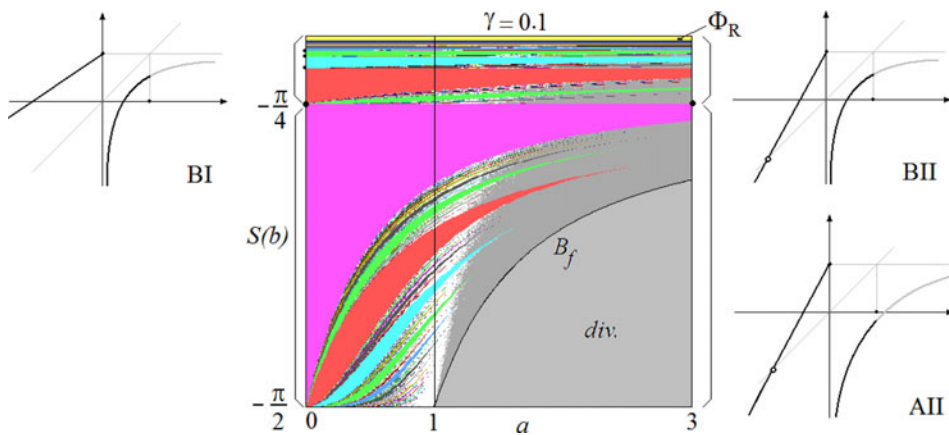


Figure 1. Two-dimensional bifurcation diagram in the parameter space  $(a, S(b))$ , at  $\gamma = 0.1, b(\Phi_R) = -0.7152667$ . The qualitative shape of  $f(x)$  in three different ranges, AII, BI and BII, is also shown.

curves of cycles having the same symbolic sequences are proved to exist, and the related properties are illustrated. They are limit points of infinite families of BCBs. Also the fold bifurcation values and the homoclinic bifurcation values are shown to be limit points of infinite families of BCB values. In Subsection 4.2 we investigate Range BII, showing that the map has properties similar to those occurring in Range AII, although now a chaotic repeller belonging to the frontier of  $B_\infty$  always exists. The basin of attraction  $B_\infty$  of positive measure may coexist with another basin of positive measure, related to an attracting cycle of period  $n \geq 1$ . The existing attracting cycles are related to periodicity regions issuing from organizing centres in Range BI. Section 5 concludes, evidencing that there are many open problems which are left for further investigation.

## 2. Preliminary properties

For the PWS map in (2), the discontinuity point is at the origin,  $x = 0$ , that is also a vertical asymptote for the function on the right side. In the parameter Range BI, in which the slope of the straight line is not larger than 1, any point on the right side, no matter how close it is to  $x = 0$ , is mapped to the left side and then the trajectories start to increase and a point with  $x > 0$  is reached again. That is, the trajectories cannot be divergent, as it also occurs in the invertible case studied in [14] and in the non-invertible case of Range AI considered in [13].

Differently, in the Ranges AII and BII, in which  $a > 1$ , due to the existence of the repelling fixed point  $x_L^*$ , the vertical asymptote is mainly related to divergent trajectories. In fact, as already recalled in the Introduction, a set of positive measure of points with divergent dynamic behaviour exists, denoted  $B_\infty$  (basin of  $-\infty$  or set of divergent trajectories). As any total basin, it is given by all the preimages of any rank of the immediate basin, which is the interval  $(-\infty, x_L^*) = (-\infty, -1/(a-1))$ , so that

$$B_\infty = \bigcup_{k=0}^{\infty} f^{-k}(-\infty, x_L^*). \quad (6)$$

Clearly, the first preimage of the immediate basin is  $f_R^{-1}((-\infty, x_L^*)) = (0, x_L^{*-1})$  which is the right neighbourhood of the origin bounded by the preimage  $x_L^{*-1} = f_R^{-1}(x_L^*)$ , given by

$$x_L^{*-1} = \left( \frac{b}{x_L^* - 1} \right)^{1/\gamma} = \left( \frac{-b(a-1)}{a} \right)^{1/\gamma}. \quad (7)$$

An immediate result is that bounded dynamics different from the preimages of the repelling fixed point  $x_L^*$  can exist only for parameter values such that  $x_L^{*-1} < 1$ , which leads to the condition  $b > -a/(a-1)$ . In the  $(a, b)$ -parameter plane the curve  $B_f$  of equation

$$B_f : b = -\frac{a}{a-1} \quad (8)$$

is below the line  $b = -1$ , independently of the value of  $\gamma > 0$ , and it bounds a region associated with only divergence. In fact, when  $x_L^{*-1} \geq 1$  ( $b \leq -a/(a-1) < -1$ ), then except for  $x_L^*$  and its preimage  $x_L^{*-1}$ , all the other points have a divergent trajectory, being mapped to the immediate basin  $(-\infty, x_L^*)$  in one or two iterations at most.

Differently, for  $b > -a/(a-1)$  a bounded chaotic set exists. To prove the existence of chaotic sets we make use of the existence of homoclinic orbits. It is well known that in

one-dimensional non-invertible maps, homoclinic orbits of a repelling  $k$ -cycle,  $k \geq 1$  ( $k = 1$  corresponds to a fixed point), exist when it is a snap-back repeller (SBR), following the definition given by Marotto in [15], [16]. We recall that a repelling cycle may become an SBR via a critical homoclinic orbit, associated with critical homoclinic explosions, or  $\Omega$ -explosions, as shown in [8] for smooth continuous systems, and in [9] for generic PWL and PWS systems, continuous and discontinuous. The existence of homoclinic orbits leads us to show that for parameter values satisfying

$$-\frac{a}{a-1} < b < 0 \tag{9}$$

a bounded chaotic repeller always exists in the interval  $[x_L^*, 1]$ , as stated in the following proposition.

**PROPOSITION 1.** (SBR bifurcation of  $x_L^*$ ). Consider map  $f(x)$  given in (2) with  $\gamma > 0$  and  $a > 1$ .

If  $-\infty < b < -a/(a-1)$  then all the points except for  $x_L^* = -1/(a-1)$  and  $x_L^{*-1} = (-b(a-1)/a)^{1/\gamma}$  have a divergent trajectory.

If  $b = -a/(a-1)$  besides  $x_L^*$ , the only non-divergent points belong to a critical homoclinic orbit of  $x_L^*$ . No chaotic repeller exists.

If  $-a/(a-1) < b < 0$  then  $x_L^*$  is an SBR and a bounded chaotic repeller exists in  $[x_L^*, 1]$ .

*Proof.* The first point is immediate, as shown above. For the third item, notice that for parameter values such that  $b > -a/(a-1)$  it is  $x_L^{*-1} < 1$ , which leads to the existence of a sequence of preimages of  $x_L^{*-1}$  from the left side. That is, for any  $k > 0$ ,

$$x_L^{*-(k+1)} = f_L^{-k}(x_L^{*-1}) \tag{10}$$

gives a sequence of points converging from above to  $x_L^*$ , leading to a non-critical (and non-degenerate) homoclinic orbit of  $x_L^*$ . Thus  $x_L^*$  is an SBR, and this is enough to state that in the interval  $[x_L^*, 1]$  a bounded chaotic set of map  $f$  exists (see [9]).

At the homoclinic bifurcation value  $b = -a/(a-1)$  it holds  $x_L^{*-1} = 1$  and thus  $f_L^{-1}(x_L^{*-1}) = 0$  so that a critical homoclinic orbit of  $x_L^*$  exists. However, all the points in  $(0, 1)$  are mapped in the immediate basin of  $B_\infty$  thus the only non-divergent points are those belonging to the homoclinic orbit, and no chaotic repeller can exist.  $\square$

It follows that an explosion of repelling cycles occurs as the parameter  $b$  increases through the value  $-a/(a-1)$ , and a parameter point  $(a, b)$  crosses the curve  $B_f$ . This global bifurcation will be explained and commented in the next section. Not only  $x_L^*$  becomes homoclinic, but also infinitely many repelling cycles, among which basic cycles  $RL^n$ , appear and are homoclinic.

Moreover, as we shall see, for  $b$  satisfying (9) the invariant set of bounded dynamics can be of positive measure or a chaotic set of zero measure. The two different behaviours depend on the existence or non-existence of an attracting cycle, respectively.

As an example of the existence of attracting cycles, in Figure 1 it is shown the two-dimensional bifurcation diagram in the parameter space  $(a, S(b))$  at the fixed value  $\gamma = 0.1$ . In order to consider the parameter space in the complete range for the parameter  $b$ , that means  $-\infty < b < 0$ , following [2] we use the nonlinear transformation  $S(y) = \arctan(y)$  which maps an unbounded interval into a bounded one. So that instead of the

interval  $b \in (-\infty, 0)$  we have the interval  $\arctan(b) \in (-\pi/2, 0)$ . In particular, in the case  $b = -1$  we have  $\arctan(-1) = -\pi/4$  which is evidenced in [Figure 1](#).

The coloured regions in [Figure 1](#) represent sets of values of the parameters for which the map has an attracting cycle, different colours are associated with different periods, showing many different periodicity regions. We also notice that cycles of the same period have a different symbolic sequence for  $b < -1$  and  $-1 < b < 0$ . White points in  $a \leq 1$  represent parameter sets at which there exists an unbounded chaotic attractor, while white points in  $a > 1$  represent parameter sets at which there exists a bounded chaotic repeller, or an attracting cycle of period larger than 45.

In the parameter region  $b < -1$  infinitely many periodicity regions are issuing from the particular point  $(a, b) = (0, -\infty)$  while in the parameter region  $-1 < b < 0$  infinitely many periodicity regions are issuing from particular codimension-two points  $(0, b(B_{LR^n}))$  which behave as organizing centres, and still to be properly investigated.

Grey regions existing for  $a > 1$  represent parameter sets at which the system has divergent trajectories (which may or may not coexist with an attracting cycle). The light grey region is bounded by the bifurcation curve  $B_f$  given in (8), and below it the dynamics are divergent, as stated in Proposition 1.

Besides the repelling fixed point  $x_L^*$ , fixed points on the right side may also exist. They are associated with a smooth fold bifurcation of the increasing branch  $f_R(x)$  of the map, so that when existing they are in pair, one attracting and one repelling. The fixed points can be obtained by solving the equation  $f_R(x) = x$ , that is

$$\frac{b}{x^\gamma} + 1 = x \quad (11)$$

whose solutions in general cannot be written in explicit form. However, we can investigate the fold bifurcation value and the value of the two merging fixed points, say  $x_R^*$ , by considering the condition that the first derivative in the fixed point must be equal to  $+1$ . Thus, from

$$f'_R(x) = \frac{-b\gamma}{x^{\gamma+1}} \quad (12)$$

by using these two conditions  $b/(x_R^*)^\gamma + 1 = x_R^*$  and  $-b\gamma/(x_R^*)^{\gamma+1} = 1$  we obtain the equation of the fold bifurcation curve

$$\Phi_R : b = b(\Phi_R), \quad b(\Phi_R) = -\frac{1}{\gamma} \left( \frac{\gamma}{\gamma+1} \right)^{\gamma+1} \quad (13)$$

and the fixed point at the fold bifurcation is given by

$$x_R^* = \frac{\gamma}{\gamma+1} < 1. \quad (14)$$

It is worth to note that for any  $\gamma > 0$  the value of  $b$  related to the fold bifurcation is always larger than  $-1$  (i.e.  $-(1/\gamma)(\gamma/(\gamma+1))^{\gamma+1} > -1$ , which is equivalent to  $\gamma^\gamma < (\gamma+1)^{\gamma+1}$ ), and that  $x_R^* < 1$ .

**PROPOSITION 2.** *Let  $\gamma > 0$ ,  $a > 0$ ,  $b(\Phi_R) < b < 0$ , then the map  $f$  has two fixed points in the  $R$  side, one repelling,  $x_R^u$  and one attracting  $x_R^s$ , satisfying  $0 < x_R^u < x_R^s < 1$ .*



*Proof.* As shown above, the branch  $f_R$  becomes tangent to the main diagonal when (13) holds, and it intersects the main diagonal in two distinct points for  $b(\Phi_R) < b < 0$ . Recall that in generic cases, a monotone increasing continuous map can only have fixed point whose stability is alternating. Since  $f'_R(x) > 0$  and  $f''_R(x) < 0$  for any  $x > 0$ , in our map  $f$  we can have only one pair of fixed points, say  $x_R^u < x_R^s$ , then the fixed point  $x_R^u$  is repelling, as the slope is larger than 1, while the opposite occurs in the fixed point  $x_R^s$ , which is thus attracting.  $\square$

The right branch of the map,  $f_R(x)$ , has horizontal asymptote at the value 1 so that any point  $x > 1$  is mapped in one iteration to a point smaller than 1. Moreover,  $f_R(x)$  intersects the  $x -$  axis in a point which is the solution of  $f_R(x) = 0$ , leading to

$$x = (-b)^{1/\gamma} =: O_R^{-1}. \tag{15}$$

This point is the rank-1 preimage of the origin (discontinuity point) on the right side, and clearly it plays an important role when  $O_R^{-1} \leq 1$ . We have  $O_R^{-1} > 1$  (respectively,  $< 1$ ) for  $b < -1$  (respectively,  $-1 < b < 0$ ). This different shape of the map on the right side, also qualitatively evidenced in Figure 1, leads to different dynamic behaviours in the PWS map  $f$ , and motivates the introduction of the different ranges, as defined in Section 1 in (3), each one considered separately in the following sections.

**3. Range AII ( $a > 1, b \leq -1$ ): mainly divergence**

As described in [13], any cycle of map  $f$  may undergo a BCB: this happens when a periodic point collides with  $x = 0$  from the left side and thus its image is a periodic point on the right side  $(0, 1]$  which collides with  $x = 1$ . In that paper we have determined the BCB curves  $B_{RL^n}$  of basic cycles of symbolic sequence  $RL^n$  occurring for  $b < -1$  that is

$$B_{RL^n} : b = -\frac{a^n - 1}{a^{n-1}(a - 1)} \tag{16}$$

as well as the fold bifurcation curves  $\Phi_{RL^n}$  of the same basic cycles, that is

$$\Phi_{RL^n} : b = -\frac{1}{\gamma a^n} \left( \frac{a^{n+1} - 1}{a - 1} \frac{\gamma}{\gamma + 1} \right)^{\gamma+1}, \quad a \leq \bar{a}_n \tag{17}$$

where  $(\bar{a}_n, \bar{b}_n), \bar{b}_n = -(1/\gamma\bar{a}_n)$  is a codimension-two point related to cycles with the same symbolic sequence  $RL^n$  (contact point between the curve  $B_{RL^n}$  and the curve  $\Phi_{RL^n}$ ). Moreover, we have seen that for any  $n > 1$ , the following inequalities hold:

$$a_\infty = \frac{1}{\gamma + 1} < \bar{a}_{n+1} < \bar{a}_n < \bar{a}_1 = \frac{1}{\gamma} \tag{18}$$

which leads to the following proposition.

**PROPOSITION 3.** *Let  $a > 1, b \leq -1$  and  $0 < \gamma < 1$ . If the codimension-two point  $(\bar{a}_n, \bar{b}_n)$  satisfies  $\bar{a}_n > 1$  then the region of an attracting cycle  $RL^n$  exists.*

*Let  $a > 1, b \leq -1$  and  $\gamma \geq 1$ , then besides divergent trajectories only a bounded chaotic repeller can exist.*

Downloaded by [93.150.144.95] at 06:43 19 June 2015

*Proof.* From (18) it is immediate that for  $\gamma \geq 1$  it holds  $\bar{a}_1 \leq 1$  so that for  $a > 1$  no fold bifurcation curve  $\Phi_{RL^n}$  can be crossed and no basic cycle can be attracting. Moreover, we have numerical evidence that also all the other existing cycles have no stability regions. Thus for  $a > 1$  the ranges in which we can have a set of positive measures of non-divergent trajectories are related to the values  $0 < \gamma < 1$ .

We know that for a fixed value of  $a, a > 1$ , increasing  $b$  from the boundary  $B_f$  when a fold bifurcation curve  $\Phi_{RL^n}$  is not crossed (for  $a > \bar{a}_n$ ), then the BCB occurring crossing  $B_{RL^n}$  involves a repelling basic cycle, while when the fold bifurcation curve  $\Phi_{RL^n}$  is crossed first (for  $a < \bar{a}_n$ ), then the BCB occurring crossing  $B_{RL^n}$  involves an attracting cycle.  $\square$

For  $0 < \gamma < 1$  at least the stability region of the 2-cycle LR exists in  $a > 1$  (since  $\bar{a}_1 = 1/\gamma > 1$ ). In the  $(a, b)$ -parameter plane,  $b = -1$  is the equation of the BCB curve of a 2-cycle, as  $f_L(0) = 1$  and  $f_R(1) = 0$  holds independently of the values of the other parameters  $a$  and  $\gamma$ . Moreover, for  $a < \bar{a}_1$  the BCB involves an attracting 2-cycle, while for  $a \geq \bar{a}_1$  it involves a repelling 2-cycle.

An important result is that to study the dynamics of map  $f(x)$  for  $x_L^{*-1} < 1$  (when divergent trajectories exist) we can still make use of a first return map inside the interval  $[0, 1]$ , similar to the one used in [13], even if there are points in  $(0, 1)$  with divergent trajectories. In fact, regarding the function on the right side, recall that in one iteration any point  $x > 1$  is mapped to a point  $f_R(x) < 1$ , so that we can study the dynamics of the map by using the first return map in  $[0, 1]$ , but considering only the first return of the points in the interval

$$J = (x_L^{*-1}, 1] \subset I = [0, 1]$$

as for the remaining points we know that the trajectory never comes back (since the interval  $(0, x_L^{*-1})$  is mapped in the immediate basin of infinity  $(-\infty, x_L^*)$ ).

The existence and construction of the first return map of  $f$  in the suitable interval are given in the following proposition.

**PROPOSITION 4.** *Let  $a > 1, \gamma > 0$  and  $-(a/(a - 1)) < b \leq -1$ . The dynamics of map  $f$  in (2) can be studied by using the first return map  $F_r(x)$  in the interval  $I = [0, 1]$ , taken for the points in the interval  $J = (x_L^{*-1}, 1]$ .  $F_r(x)$  is a discontinuous map with infinitely many branches defined as follows:*

$$F_r(x) := \begin{cases} F_{RL^{\bar{n}}}(x) = f_L^{\bar{n}} \circ f_R(x) & \text{if } \xi_{\bar{n}+1} \leq x \leq 1 \\ F_{RL^{\bar{n}+1}}(x) = f_L^{\bar{n}+1} \circ f_R(x) & \text{if } \xi_{\bar{n}+2} \leq x < \xi_{\bar{n}+1} \\ \vdots & \vdots \\ F_{RL^{\bar{n}+j}}(x) = f_L^{\bar{n}+j} \circ f_R(x) & \text{if } \xi_{\bar{n}+j+1} \leq x < \xi_{\bar{n}+j} \\ \vdots & \vdots \end{cases} \quad (19)$$

where  $\bar{n} \geq 1$  is the smallest integer for which  $f_L^{\bar{n}} \circ f_R(1) \in [0, 1)$ ,

$$F_{RL^m}(x) = \frac{a^m b}{x^\gamma} + \frac{1 - a^{m+1}}{1 - a}$$

and the discontinuity points are preimages of the origin given by

$$\xi_{m+1} = f_R^{-1} \circ f_L^{-m}(0) = \left( \frac{-b}{((a^m - 1)/(a^m(a - 1))) + 1} \right)^{1/\gamma} \tag{20}$$

which have as limit value, as  $m \rightarrow \infty$ , the point  $x_L^{*-1}$ .

Moreover, for any  $j \geq 1$ ,  $F_{RL^{\bar{n}+j}}(\xi_{\bar{n}+j+1}) = 0$  and  $F_{RL^{\bar{n}+j}}(\xi_{\bar{n}+j}) = 1$  hold, while the rightmost branch satisfies  $F_{RL^{\bar{n}}}(\xi_{\bar{n}+1}) = 0$  and its range can be smaller than  $[0, 1]$ .

*Proof.* Starting from the first return of the point  $x = 1$ , let  $\bar{n}$  be the smallest integer such that

$$f_L^{\bar{n}} \circ f_R(1) \in [0, 1] \tag{21}$$

then  $F_r(x)$  is necessarily defined as in (19). The infinitely many preimages  $f_L^{-m}(0)$  of 0 exist for any  $m \geq 1$ , and have as limit set the repelling fixed point  $x_L^*$ . Thus the infinitely many preimages  $\xi_{m+1} = f_R^{-1} \circ f_L^{-m}(0)$ , discontinuity points of  $F_r(x)$ , also exist in the interval  $(x_L^{*-1}, 1]$  for any  $m \geq \bar{n} + 1$ , and have  $x_L^{*-1}$  as limit point.

In the particular case in which the condition in (21) occurs as  $f_L^{\bar{n}} \circ f_R(1) = 0$ , we also have  $F_{RL^{\bar{n}+1}}(x) = f_L^{\bar{n}+1} \circ f_R(1) = 1$ , so that we define  $F_r(1) = f_L^{\bar{n}} \circ f_R(1) = 0$  in the single point  $\xi_{\bar{n}+1} = 1$  and  $F_r(x) = f_L^{\bar{n}+1} \circ f_R(x)$  in  $[\xi_{\bar{n}+2}, \xi_{\bar{n}+1})$ . Notice that in this case the range of  $F_{RL^{\bar{n}+1}}(x) = f_L^{\bar{n}+1} \circ f_R(x)$  in  $[\xi_{\bar{n}+2}, 1]$  is exactly  $[0, 1]$ , and similarly in all the other branches of  $F_r(x)$  which are defined in (19).  $\square$

An example is shown in Figure 2. For  $x = 1$  we have  $f_L^4 \circ f_R(1) > 0$  so that  $\bar{n} = 4$ . The preimages of the origin on the left side are accumulating to  $x_L^*$  and a few of the infinitely many branches of  $F_r(x)$  (accumulating to  $x_L^{*-1}$ ) can be seen in the enlargement.

The particular case

$$f_L^{\bar{n}} \circ f_R(1) = 0 \tag{22}$$

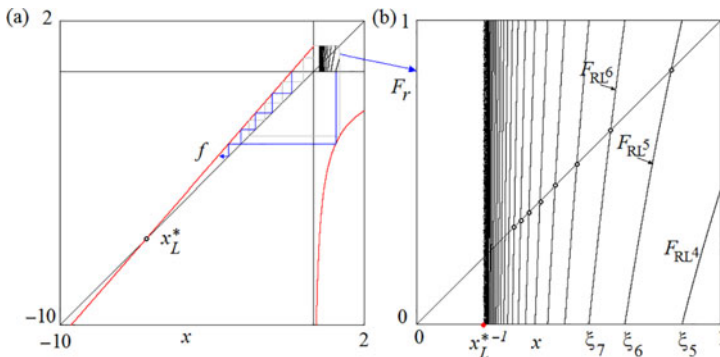


Figure 2. In (a) map  $f(x)$  is shown at  $\gamma = 0.5$ ,  $a = 1.15$ ,  $b = -3.6$ , for which it is  $\bar{n} = 4$ , and its first return map  $F_r(x)$  in  $[0, 1]$  is also shown. In (b) map  $F_r(x)$  is enlarged. The discontinuity points  $\xi_j$  have limit point  $x_L^{*-1} = 0.22049$ .

mentioned in the proof given above can be rewritten as  $f_L^{\bar{n}} \circ f_R \circ f_L(0) = 0$  (since  $f_L(0) = 1$ ), or equivalently, by applying  $f_L$  on both sides of (22), as follows:

$$F_{RL^{\bar{n}+1}}(1) = f_L^{\bar{n}+1} \circ f_R(1) = 1 \tag{23}$$

and thus it corresponds to the BCB of a basic cycle with symbolic sequence  $RL^{\bar{n}+1}$  (as in fact  $x = 0$ , as well as  $x = 1$ , is a periodic point of period  $(\bar{n} + 2)$ ).

In terms of the preimages of the origin the condition in (22) also corresponds to

$$1 = f_R^{-1} \circ f_L^{-\bar{n}}(0) \tag{24}$$

and by using the definition in (20) with  $m = \bar{n}$ ,  $\xi_{\bar{n}+1} = 1$ , after some algebra we get the equation of the BCB of a cycle with symbolic sequence  $RL^{\bar{n}}$  given in (16).

We can also notice that each component of the first return map  $F_r$ ,  $F_{RL^n}(x)$  is continuous and increasing, as  $F'_{RL^n}(x) > 0$ , for  $x > 0$ . This also follows from the explicit expression of the first derivative:

$$F'_{RL^n}(x) = a^n f'_R(x) = \frac{-b\gamma}{x^{\gamma+1}} a^n > 0. \tag{25}$$

Moreover, since  $F''_{RL^n}(x) < 0$ , for  $x > 0$ , as follows from

$$F''_{RL^n}(x) = \frac{d}{dx} \left( \frac{-b\gamma}{x^{\gamma+1}} a^n \right) = \frac{b\gamma(\gamma+1)}{x^{\gamma+1}} a^n < 0 \tag{26}$$

all the branches are concave. The range of each component is from 0 to 1, except at most the first branch on the right, called rightmost branch. It is worth noticing that the properties of increasing and concave branches hold for any composition of the functions  $F_{RL^n}(x)$ .

Another immediate consequence of the constructive definition of the first return map  $F_r(x)$ , is that infinitely many repelling basic cycles necessarily exist. In fact, for any  $j \geq \bar{n} + 1$  the increasing and concave branches  $F_{RL^j}(x)$  which are continuous and take values from 0 to 1 lead to repelling fixed points  $x_{RL^j}$ , and it is easy to see that all these points are homoclinic.

Since the interval  $(0, x_L^{*-1})$  represents a set of points having divergent trajectories, then also all the points in  $J = (x_L^{*-1}, 1]$  which are mapped in the interval  $(0, x_L^{*-1})$  will have divergent trajectories too. So it is clear that for  $x_L^{*-1} < 1$  there are infinitely many intervals in  $J$  which are preimages of some rank of  $(0, x_L^{*-1})$  and thus belong to the basin  $B_\infty$ . However, what is left can be a set of positive measure or of zero measure, and the map  $F_r(x)$  completely represents the dynamics of  $f$ . The two possible dynamic behaviours so described are illustrated in Figures 2 and 3.

At the parameter values used in Figure 2, it is  $x_L^{*-1} = 0.153119$  and  $\bar{n} = 4$ , so that the rightmost branch of the first return map is given by  $F_{RL^4}(x)$  in the interval  $[\xi_5, 1]$ . All the other preimages  $\xi_j$ , discontinuity points of  $F_r(x)$ , exist for any  $j > 5$  accumulating to  $x_L^{*-1}$ . Thus, also all the branches defined by  $F_{RL^{4+j}} = f_L^{4+j} \circ f_R(x)$  exist for any  $j \geq 1$  and intersect the diagonal, leading to the existence of repelling (SBR) fixed points  $x_{RL^j}$  for any  $j > 5$ , which also are accumulating to  $x_L^{*-1}$ , and are associated with basic cycles of  $f$ . From the shape of the branches of  $F_r$  we can see that in this case no attracting cycle can exist (as the slope of  $F_r$  is everywhere larger than 1). A chaotic repellor  $\Lambda$  exists in the interval  $(x_L^{*-1}, 1]$  which includes all the repelling cycles, their stable sets and related limit points. Taking the preimages by  $F_r(x)$  of the interval  $(0, x_L^{*-1})$  we can see that almost all the points of the

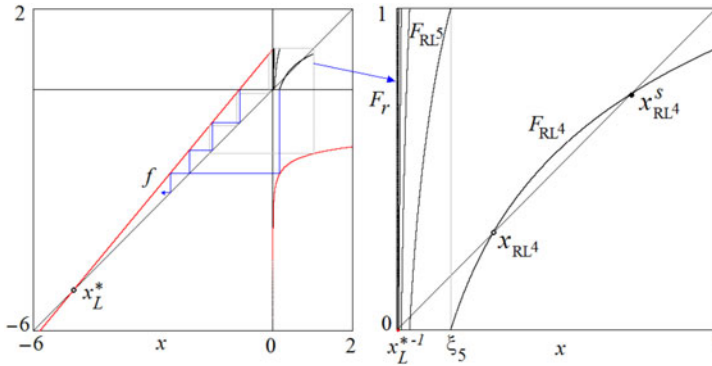


Figure 3. In (a) map  $f(x)$  is shown at  $\gamma = 0.5$ ,  $a = 1.2$ ,  $b = -2.6$ , for which it is  $\bar{n} = 4$ , and its first return map  $F_r(x)$  in  $[0, 1]$  is also shown. In (b) map  $F_r(x)$  is enlarged. The discontinuity points  $\xi_j$  have limit point  $x_L^{*-1} = 0.0002335$ .

interval  $(x_L^{*-1}, 1]$  belong to the basin  $B_\infty$ . These preimages form a fractal structure, and are dense in the interval  $(x_L^{*-1}, 1]$ , and the frontier is given by the chaotic repeller  $\Lambda$ . For the map  $f$  this means that a chaotic repeller belongs to  $[x_L^*, 1]$  and all the other points have divergent trajectories.

Moreover, as  $b$  increases from the value  $-3.6$ , used in Figure 2, the value  $F_{RL^4}(1) = f_L^4 \circ f_R(1)$  of the rightmost branch of  $F_r$  increases, and when  $F_{RL^4}(1) = f_L^4 \circ f_R(1) = 1$ , from (23) it follows that the BCB of the cycle with symbolic sequence  $RL^4$  occurs (and from (16) with  $a = 1.15$  and  $n = 4$  the bifurcation value  $b \approx -3.2832$  is obtained). Differently, as  $b$  decreases from the value  $-3.6$ , the value  $F_{RL^4}(1) = f_L^4 \circ f_R(1)$  of the rightmost branch of  $F_r$  decreases, and when  $F_{RL^4}(1) = f_L^4 \circ f_R(1) = 0$  (which corresponds to  $f_L^5 \circ f_R(1) = 1$ ) from (22) it follows that the BCB of the cycle with symbolic sequence  $RL^5$  occurs (and from (16) with  $a = 1.15$  and  $n = 5$  the bifurcation value  $b \approx -3.855$  is obtained). As  $b$  decreases up to the boundary of the curve  $B_f$ , which occurs at  $b = -a/(a - 1) = -7.\bar{6}$ , all the BCB curves of cycles with symbolic sequence  $RL^k$  for  $k > 4$  are crossed, as in fact the limit set, point  $x_L^{*-1}$  (given in (7)), approaches the value  $x = 1$ . Thus, in the example given in Figure 2 for any  $b \in (-7.\bar{6}, -3.6)$  the non-divergent set is always a bounded chaotic repeller, the segments of points having divergent trajectories become wider and wider as  $b$  decreases, and for  $b = -a/(a - 1) = -7.\bar{6}$  any orbit is divergent except for a unique homoclinic orbit of  $x_L^*$  (Proposition 1).

Differently, at the parameter set used in Figure 3, we have  $x_L^{*-1} = 0.0002335$ , and since  $\bar{n} = 4$  the rightmost branch of the first return map is given by  $F_{RL^4}(x)$  in the interval  $[\xi_5, 1]$ . All the other preimages  $\xi_j$ , discontinuity points of  $F_r(x)$ , exist for any  $j > 5$  accumulating to  $x_L^{*-1}$ . Thus, also all the repelling (SBR) fixed points  $x_{RL^j}$  exist for any  $j > 5$ , accumulating to  $x_L^{*-1}$ , basic cycles of  $f$ . From the shape of the branches of  $F_r$  now we can see that in this case an attracting cycle exists, as the rightmost branch  $F_{RL^4}(x)$  intersects the diagonal in two fixed points, one repelling ( $x_{RL^4}$ ) and the other attracting ( $x_{RL^4}^s$ ), with  $\xi_5 < x_{RL^4} < x_{RL^4}^s < 1$  (which are basic cycles of  $f$  both with symbolic sequence  $RL^4$ ). The immediate basin of the attracting fixed point  $x_{RL^4}^s$  is the interval  $(x_{RL^4}, 1]$ , and the total basin, of positive measure, is the set of all its preimages, which has a fractal structure, as its frontier includes a chaotic repeller  $\Lambda'$  which consists of all the repelling cycles, their stable sets and related limit points. Clearly there is also another basin of positive measure, that of points having divergent trajectories, given by the interval  $(0, x_L^{*-1})$  and all its preimages in the interval  $(x_L^{*-1}, 1]$ , which also has a fractal structure.

The frontier between the two basins of positive measure is given by all the preimages of the point  $x_L^{*-1}$  (which are dense in the chaotic repeller  $\Lambda'$ ).

For the map  $f$  this means that a chaotic repeller belongs to  $[x_L^*, 1]$  and separates two basins of attraction, both of positive measure, one is  $B_\infty$  and the other is the basin  $B(x_{RL}^s)$ .

For  $a > 1$  we can take advantage of other results obtained in [13], as it is easy to see that they hold also in Range AII. In fact, the equations of the BCB curves  $B_{RL^n}$  reported in (16) and fold bifurcation curves  $\Phi_{RL^n}$  in (17) are clearly unchanged, and unchanged are also their properties related to the dynamics when the BCB curves are crossed in the  $(a, b)$ -parameter plane. The codimension-two point  $(\bar{a}_n, \bar{b}_n)$  on a BCB curve  $B_{RL^n}$  separates different dynamic behaviours. When the parameter point  $(a, b)$  belongs to the BCB curve  $B_{RL^n}$  then a periodic point is merging with  $x = 1$ , for the rightmost branch of the first return map it holds  $F'_{RL^n}(1) = -b\gamma a^n = \gamma a^n \frac{a^n - 1}{a^{n-1}(a-1)} = \gamma a \frac{a^n - 1}{a-1}$  and

- for  $a < \bar{a}_n$  it holds  $F'_{RL^n}(1) < 1$  which means that the colliding cycle is attracting, and thus the fold bifurcation curve  $\Phi_{RL^n}$  (associated with a point in which  $F'_{RL^n} = 1$ ) must have been crossed before at a smaller value of  $b$ ;
- for  $a > \bar{a}_n$  it holds  $F'_{RL^n}(1) > 1$  which means that the colliding cycle is repelling, and thus the fold bifurcation curve  $\Phi_{RL^n}$  is not involved (it is virtual).

For a point  $(a, b) \in B_{RL^n}$  with  $a \geq \bar{a}_n$ , the first return map consists of infinitely many branches  $F_{RL^j}(x), j \geq n$ , and all of them, including the rightmost one  $F_{RL^n}(x)$ , have range  $[0, 1]$ . Since  $F'_{RL^n}(1) > 1$ , then it must be  $F'_{RL^n}(x) > 1$  for any  $x \in [\xi_{n+1}, 1)$ . Notice that the codimension-two points  $\bar{a}_j$  of  $B_{RL^j}(x), j > n$ , are all smaller than  $\bar{a}_n$  which means that at fixed  $a$  decreasing  $b$  all the BCB curves  $B_{RL^j}(x), j > n$  are crossed and at such bifurcation points it holds  $F'_{RL^j}(1) > 1$  for any  $j > n$ . This implies that at  $(a, b) \in B_{RL^n}$  also all the other branches, given by  $F_{RL^j}(x), j > n$ , are expansive. In fact, the slope is certainly  $F'_{RL^j}(x) > 1$  for  $x \in [\xi_{j+1}, x_{j+1}^*]$  where  $x_{j+1}^*$  is the repelling fixed point of  $F_r(x)$ , then for  $x \in [x_{j+1}^*, \xi_j]$  the slope, although decreasing, is larger than 1 as at the considered parameter value of  $a$  it cannot cross the value 1 (a branch  $F_{RL^j}(x)$  of the first return map can have points with slope smaller than 1 only if at fixed value of  $a$ , decreasing  $b$  the fold bifurcation curve  $\Phi_{RL^j}$  is crossed, which can occur for  $a < \bar{a}_j$  that cannot be at the considered parameter value).

The above arguments show that the first return map is expanding at the points  $(a, b) \in B_{RL^j}$  (where  $a \geq \bar{a}_n$ ) for any  $j \geq n$ , so that the non-divergent set is a bounded chaotic repeller. The same result holds not only at the BCB values. In fact, considering any point  $(a, \bar{b}) \in B_{RL^n}$  with  $a > \bar{a}_n$ , above the curve  $B_f$ , then for any parameter point  $(a, b)$  with  $-a/(a-1) < b \leq \bar{b}$  it is  $F'_r(1) > 1$  and thus the rightmost branch of  $F_r(x)$  has the slope larger than 1 in all its points (due to monotonicity and concavity), as in the example shown in the enlargement of Figure 2. Then, not only the rightmost branch, but also all the other (infinitely many) branches defining the first return map  $F_r(x)$  have the slope larger than 1 in all the points. In fact, reasoning as above, the related branches all have a repelling fixed point, with slope larger than 1, and on its right side the slope, although decreasing, cannot cross the value 1 (as this cannot occur for the considered parameter values  $\bar{a} > \bar{a}_n$ ).

We have so proved that for any fixed  $\gamma > 0$  considering a BCB curve  $B_{RL^n}$ , in all the points  $(a, b)$  of the two-dimensional bifurcation diagram with  $a \geq \bar{a}_n$  and  $b \leq \bar{b}_n$  above the curve  $B_f$ , the first return map  $F_r(x)$  is expanding, and thus the non-divergent set is always a bounded chaotic repeller. As a parameter point  $(a, b)$  approaches the curve  $B_f$  all the repelling fixed points of  $F_r(x)$  approach the limit point  $x_L^{*-1}$  and the segments of points having divergent trajectories become wider and wider as  $b$  decreases. At the boundary of the curve  $B_f$  (at  $b = -a/(a-1)$ ) any orbit is divergent except for a unique homoclinic

orbit of  $x_L^*$  (Proposition 1). An example of the map when the parameters are approaching the curve  $B_f$  is shown in Figure 4, clearly the first integer  $\bar{n}$  is very large,  $x_L^{*-1}$  is close to 1, and all the branches constituting  $F_r(x)$  are expanding.

Only the basic cycle RL can be stable, as  $\bar{a}_1 = 2$  and  $\bar{a}_j < 1$  for  $j > 1$ . In black some BCB curves  $B_{RL^n}$  are shown. The curve  $B_f$  bounds the region of divergence without chaos (light grey points). In (b) only the bifurcation curves  $\Phi_{RL}$  (fold of the 2-cycle) and  $B_{RL^n}$  are drawn, by using the equations given in the text.

Several basic cycles  $RL^n$  can be stable (some periodicity regions are in colour), as  $\bar{a}_1 = 10$  and  $\bar{a}_j > 1$  for  $j = 1, 2, \dots, 6$ . Some BCB curves  $B_{RL^n}$  (in black) and some fold bifurcation curves  $\Phi_{RL^n}$  are also shown. The curve  $B_f$  bounds the region of divergence without a chaotic set. In (b) only the bifurcation curves  $\Phi_{RL^n}$  (in red) and  $B_{RL^n}$  (in black) are drawn, by using the equations given in the text.

It is plain that for  $a > 1$  the possibility to have periodicity regions of attracting cycles is much reduced. For example we have seen above that it is impossible for values  $\gamma \geq 1$ . However, at small values of  $\gamma$  (see Figure 1) we can have wide regions of attracting cycles also for  $a > 1$ . Two examples are illustrated in Figure 5 at  $\gamma = 0.5$  and Figure 6 at  $\gamma = 0.1$ . The green curve represents the boundary  $B_f$  of the region leading to no chaos and almost all divergent orbits.

All the BCB curves of basic cycles  $RL^n$  exist in the region above  $B_f$  and are accumulating to  $B_f$ . Also notice that the curve  $B_f$  has limit  $-\infty$  for  $a \rightarrow 1$  and limit 1 for  $a \rightarrow \infty$  (as clearly visible in Figure 1).

The curves associated with the basic cycles are shown in Figures 5 and 6, but there are infinitely many other BCB curves, dense in the region above  $B_f$ . The existence of fold bifurcation curves mainly depends on the parameter  $\gamma$ . As already remarked, they do not exist for  $\gamma \geq 1$ . We know that at  $\gamma = 0.5$  only the fold bifurcation curve of the 2-cycle RL exists for  $a > 1$ , as its codimension-two point is  $\bar{a}_1 = 2$ , and that of the 3-cycle  $RL^2$  is  $\bar{a}_2 = 1$ . Differently, at  $\gamma = 0.1$  we can see in Figure 6 several stability regions (in colour), thus bounded by fold bifurcation curves, at least in a right neighbourhood of  $a = 1$ .

The dark grey points in the two-dimensional bifurcation diagrams in Figures 5 and 6 denote that the initial condition used in the numerics belongs to  $B_\infty$ .

When a parameter point  $(a, b)$  (at fixed  $\gamma < 1$ ) belongs to a periodicity region related to an attracting basic cycle  $RL^n$  (as in the case considered above, in Figure 3), then the

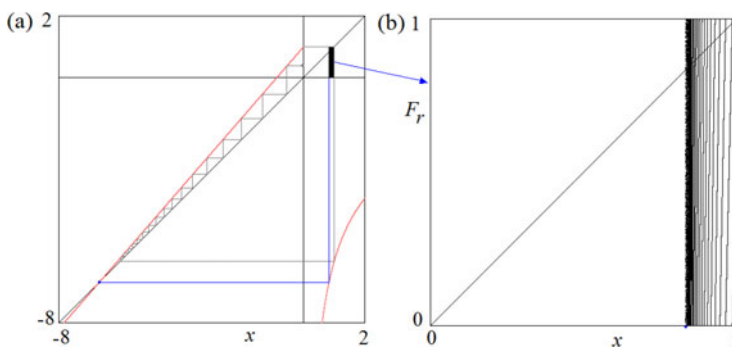


Figure 4. In (a) map  $f(x)$  is shown at  $\gamma = 0.5$ ,  $a = 1.15$ ,  $b = -7$ , for which it is  $\bar{n} = 4$ , and its first return map  $F_r(x)$  in  $[0, 1]$  is also shown. In (b) map  $F_r(x)$  is enlarged. The discontinuity points  $\xi_j$  have limit point  $x_L^{*-1} = 0.8336$ .



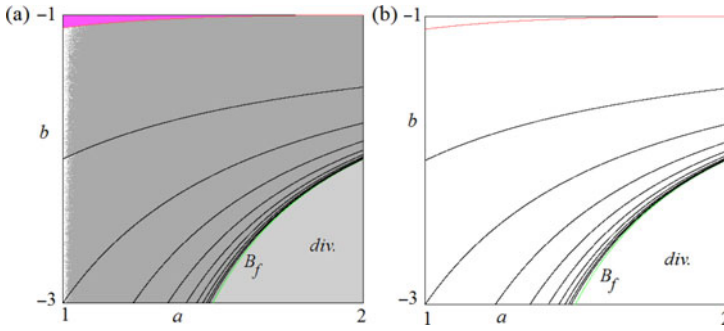


Figure 5. Two-dimensional bifurcation diagram in the  $(a, b)$ -parameter plane at  $\gamma = 0.5$ . Only the basic cycle  $RL$  can be stable, as  $\bar{a}_1 = 2$  and  $\bar{a}_j < 1$  for  $j > 1$ . In black some BCB curves  $B_{RL^n}$  are shown. The curve  $B_f$  bounds the region of divergence without chaos (light grey points). In (b) only the bifurcation curves  $\Phi_{RL}$  (fold of the 2-cycle) and  $B_{RL^n}$  are drawn, by using the equations given in the text.

rightmost branch crosses the diagonal, and two fixed points exist in the rightmost branch  $F_r(x) = F_{RL^n}(x)$ ,  $x_{RL^n}$  repelling and  $x_{RL^n}^s$  attracting, satisfying  $\xi_{n+1} < x_{RL^n} < x_{RL^n}^s < 1$ . Thus in  $J$  a set of points of positive measure exists whose trajectories converge to the attracting fixed point  $x_{RL^n}^s$ . However, the map has still a chaotic repellor, as all the repelling fixed points are homoclinic, as well as homoclinic are all the existing repelling cycles. For the first return map, the interval  $(x_{RL^n}, 1]$  is the immediate basin of the attracting fixed point  $x_{RL^n}^s$ . The total basin  $B(x_{RL^n}^s)$  is given by all the preimages of any rank of the immediate basin:

$$B(x_{RL^n}^s) = \bigcup_{k=0}^{\infty} F_r^{-k}((x_{RL^n}, 1]). \tag{27}$$

The fixed point  $x_{RL^n}$  is homoclinic on its left side while all the other fixed points  $x_{RL^j}, j > n$  (having as limit set  $x_L^{*-1}$ ) are homoclinic on both sides, so that a chaotic repellor  $\Lambda$  (an

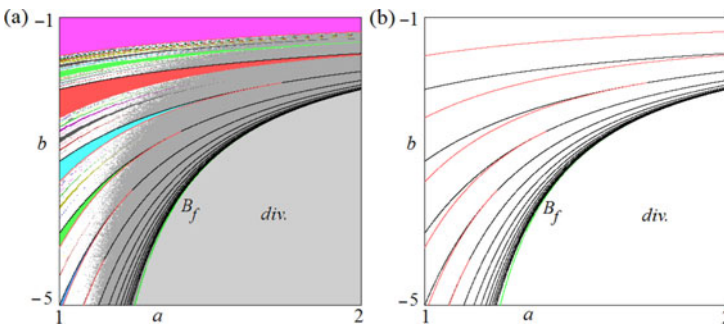


Figure 6. Two-dimensional bifurcation diagram in the  $(a, b)$ -parameter plane at  $\gamma = 0.1$ . Several basic cycles  $RL^n$  can be stable (some periodicity regions are in colour), as  $\bar{a}_1 = 10$  and  $\bar{a}_j > 1$  for  $j = 1, 2, \dots, 6$ . Some BCB curves  $B_{RL^n}$  (in black) and some fold bifurcation curves  $\Phi_{RL^n}$  are also shown. The curve  $B_f$  bounds the region of divergence without a chaotic set. In (b) only the bifurcation curves  $\Phi_{RL^n}$  and  $B_{RL^n}$  (in black) are drawn, by using the equations given in the text.



invariant Cantor set with chaotic dynamics) exists in  $[x_L^{*-1}, x_{RL^n}]$ . Thus, the total basin  $B(x_{RL^n}^s)$  consists of intervals forming a fractal structure dense in  $[x_L^{*-1}, 1]$ , its frontier  $\partial B(x_{RL^n}^s)$  includes all the repelling cycles of  $F_r$  in  $[0, 1]$ , and their limit points, that is,  $\partial B(x_{RL^n}^s)$  is the chaotic repeller  $\Lambda \subset [x_L^{*-1}, x_{RL^n}]$ . In terms of the original map  $f$  the chaotic repeller belongs to the interval  $(x_L^*, x_{RL^n}]$ , and separates two basins of positive measure,  $B_\infty$  and  $B(x_{RL^n}^s)$ .

Proposition 1 states that for  $-\infty < b \leq -a/(a - 1)$  divergent dynamics occur and a chaotic set does not exist, while for  $-a/(a - 1) < b < -1$  the map is chaotic and we have proved the following proposition.

**PROPOSITION 5.** *Let  $a > 1$  and  $0 < \gamma < 1$ , then the dynamics of map  $f$  can be classified as follows:*

- (j.1) *for  $-a/(a - 1) < b < -1$  and  $(a, b)$  not belonging to the stability region of some attracting cycle, almost all the trajectories are divergent, except for a chaotic repeller included in the interval  $[x_L^*, 1]$ ;*
- (j.2) *for  $-a/(a - 1) < b < -1$  and  $(a, b)$  belonging to the stability region of some attracting cycle with symbolic sequence  $\sigma$ , there exist two basins of positive measure. The basin  $B(x_\sigma^s) = \bigcup_{k=0}^\infty f^{-k}((x_\sigma, 1])$  where  $x_\sigma$  and  $x_\sigma^s$  are the two rightmost periodic points of the repelling and attracting cycles, respectively. The basin of divergent trajectories is given by  $B_\infty = \bigcup_{k=0}^\infty f^{-k}((-\infty, x_L^*))$ . The frontier between the two basins belongs to a chaotic repeller included in the interval  $[x_L^*, x_\sigma]$ .*

We notice that the proper structure of the existing periodicity regions of attracting or repelling cycles is still an open problem. However, what is proved is that for any fixed value  $a > 1$ , increasing the parameter  $b$  from the boundary value on the curve  $B_f$  all the BCB curves of basic cycles  $RL^n$  are crossed (the BCB of the 2-cycle  $RL$  occurs at  $b = -1$ ). Moreover, independently of the crossing also of a fold bifurcation curve of some cycle (which has the same symbolic sequence of a companion existing repelling cycle), at the value  $b = -1$  all the cycles having symbolic sequence obtained concatenating sequences of the kind  $RL^n$ , that is  $RL^{k_1}RL^{k_2}RL^{k_3} \dots$  all exist and are repelling, persisting for any larger value of  $b$ ,  $-1 < b < 0$ .

Considering the rightmost branch of the first return map  $F_r(x)$ ,  $F_{RL^n}(x)$ , we have that

- whenever  $F_{RL^n}(1)$  merges with a preimage of a discontinuity point of  $F_r(x)$  the BCB of some cycle occurs;
- whenever  $F_{RL^n}(1)$  merges with a preimage of a repelling cycle of  $F_r(x)$  one more homoclinic explosion of that cycle occurs.

So, for any fixed value of  $a$ , in any interval between two BCB curves of basic cycles,  $b(B_{RL^{n+1}}) \leq b \leq b(B_{RL^n})$ , infinitely many BCBs of cycles and homoclinic bifurcations of repelling cycles occur. In fact, increasing  $b$  in that interval, the rightmost branch of the first return map,  $F_{RL^n}(x)$ , has  $F_{RL^n}(1)$  which takes all the values from 0 to 1, crossing the values of infinitely many preimages of the discontinuity points  $\xi_j, j > n$ , accumulating to  $x_L^{*-1}$ , as well as crossing the values of infinitely many preimages of the expanding fixed points  $x_{RL^j}$ ,  $j > n$ , also accumulating to  $x_L^{*-1}$ .

#### 4. Range B ( $-1 < b < 0$ )

In the previous section we have shown that a characteristic property of the map in the range  $b < -1$  is that a point belonging to  $[0, 1]$  in the  $R$  side is immediately mapped to the

$L$  side, in one iteration. In particular, the basic cycles existing in range A are only those of symbolic sequence  $RL^n$ . In this section we consider the other range of interest, which is characterized by trajectories which can also be repeatedly mapped in the  $R$  side, and we show the existence of periodicity regions associated with attracting basic cycles having the symbolic sequence  $LR^n$  for any  $n \geq 2$ . A few of the related regions are shown in Figure 7. In fact, for the range of  $b$  here considered it holds that the preimage of the origin, say  $\xi_1 = f_R^{-1}(0) = O_R^{-1}$ , (see (15)) satisfies

$$\xi_1 = (-b)^{1/\gamma} < 1$$

so that an orbit of map  $f$  starting from a point in the interval  $(\xi_1, 1]$  must have at least two consecutive points in  $I_R$ .

We have also seen that at  $b = -1$  a border collision of a 2-cycle  $LR$  occurs, and depending on the value of  $a$ , it can be attracting or repelling.

For  $0 < a < \bar{a}_1 = 1/\gamma$  a pair of 2-cycle appears by fold bifurcation when  $b < -1$ , and the attracting one undergoes a BCB at  $b = -1$ , leaving the repelling 2-cycle, which persists (repelling) for any larger value of  $b$ .

For  $a \geq \bar{a}_1 = 1/\gamma$  at  $b = -1$  a repelling 2-cycle appears by BCB, which persists (repelling) for any larger value of  $b$ .

Moreover, for any  $a > 0$ , not only the repelling 2-cycle persists for  $b > -1$ , but also all the cycles having symbolic sequence obtained concatenating sequences of the kind  $RL^{k_1}RL^{k_2}RL^{k_3} \dots$  all exist and are repelling, persisting for any larger value of  $b$ ,  $-1 < b < 0$ .

In Section 2 we have also seen that a fold bifurcation in  $f_R$  occurs, leading to two fixed points of map  $f$ . It is worth to note that this fold bifurcation in  $f_R$  occurs independently of the value of the parameter  $a$ . That is, whichever is the value of the parameter  $a$ , as  $b$  increases from the value  $-1$  the fold bifurcation value  $b(\Phi_R)$  in (13) is reached and for  $b(\Phi_R) < b < 0$  the branch  $f_R$  intersects the main diagonal in two distinct fixed points of  $f$ ,  $x_R^u < x_R^s$ , the smallest one is repelling and the largest one attracting.

We can prove that for any fixed value of  $a > 0$  and  $\gamma > 0$  in the interval  $-1 < b < b(\Phi_R)$  the BCB curves (in the  $(a, b)$ -parameter plane) of all the basic cycles  $R^nL$  must be crossed. In fact, from  $f_R(1) = 1 + b$  we have that increasing the value of the parameter  $b$  the value  $f_R(1)$  also increases, so that when the condition  $f_R(1) = \xi_1$  holds, it corresponds to  $f_R(1) = f_R^{-1}(0)$  that is  $f_R^2(1) = 0$  and thus  $f_L \circ f_R^2(1) = 1$  or also  $f_R^2 \circ f_L(0) = 0$  leading to

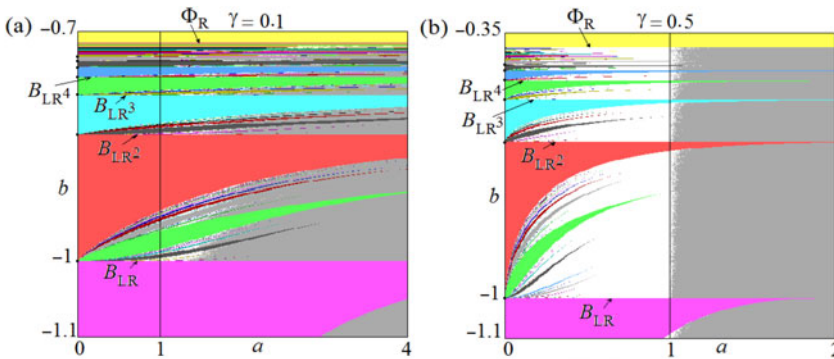


Figure 7. Two-dimensional bifurcation diagrams in the  $(a, b)$ -parameter plane. In (a)  $\gamma = 0.1$ . In (b)  $\gamma = 0.5$ .

the BCB of a 3-cycle with symbolic sequence LR<sup>2</sup>. Similarly, increasing  $b$  all the conditions

$$f_R^k(1) = \xi_1 \tag{28}$$

(i.e.  $f_R^k(1) = f_R^{-1}(0)$ ) for any  $k > 1$  must occur before the fold bifurcation value  $b(\Phi_R)$  leading to the BCB of a  $(k + 2)$ -cycle with symbolic sequence LR <sup>$k+1$</sup> . The equation of the bifurcation curve is given by

$$B_{LR^{k+1}} : f_R^{k+1} \circ f_L(0) = 0 \tag{29}$$

or equivalently, by using  $f_L(0) = 1$ ,

$$B_{LR^{k+1}} : f_L \circ f_R^{k+1}(1) = 1 \tag{30}$$

which also corresponds to

$$B_{LR^{k+1}} : f_R^{k+1}(1) = 0 \tag{31}$$

showing that the equation of the BCB of basic cycles LR <sup>$n$</sup>  is independent of the parameter  $a$ , so that in the  $(a, b)$ -parameter plane the curves are horizontal straight lines. For example, in the case  $k = 1$  (i.e. for the 3-cycle discussed above), from  $f_R(1) = 1 + b$ , and  $f_R^2(1) = f_R(1 + b) = b / ((b + 1)^\gamma) + 1$  we obtain

$$\frac{b}{(b + 1)^\gamma} + 1 = 0$$

that is  $b + (b + 1)^\gamma = 0$ . For  $\gamma = 0.5$  (as in the example shown in Figure 7(b)) we get  $b(B_{LR^2}) = ((1 - \sqrt{5})/2) \cong -0.618034$ .

We have so proved the following proposition.

**PROPOSITION 6.** *Let  $a > 0$ ,  $\gamma > 0$  and  $-1 \leq b < b(\Phi_R) = (-1/\gamma)(\gamma/(\gamma + 1))^{\gamma+1}$ . Then increasing  $b$  from  $-1$  the BCB of an  $(n + 1)$ -cycle with symbolic sequence LR <sup>$n$</sup>  for any  $n \geq 1$  occurs when the following condition, independent of  $a$ , holds:*

$$B_{LR^n} : f_R^n(1) = 0. \tag{32}$$

Moreover, at a fixed value of the parameter  $a$ , denoting  $b(B_{LR^n})$  the value of the parameter  $b$  at which the BCB curve  $B_{LR^n}$  is crossed, then the sequence  $\{b(B_{LR^n})\}_{n=1}^{n=\infty}$  is monotone increasing, i.e.  $b(B_{LR^n}) < b(B_{LR^{n+1}})$ , with limit value  $b(\Phi_R)$  as  $n \rightarrow \infty$ .

A few BCB curves at different values of  $\gamma$  are shown in Figure 7, in the  $(a, b)$ -parameter plane (horizontal straight lines). In the result proved so far we do not specify whether the BCB occurs for an attracting cycle or for a repelling one. Indeed, besides  $\gamma$ , this depends on the fixed value of the parameter  $a$ , and we shall consider below different ranges for it, that is, we shall consider separately the cases  $0 < a \leq 1$  and  $a > 1$ .

**4.1 Range BI ( $-1 \leq b < 0$ ,  $0 < a \leq 1$ ): bounded dynamics, codimension-two points of BCB and fold bifurcation**

The relevant property characterizing the range under consideration is that the left branch  $f_L(x)$  is a straight line with slope not larger than 1, so that any point on the  $L$  side has an

Downloaded by [93.150.144.95] at 06:43 19 June 2015

increasing trajectory up to a point on the  $R$  side, not larger than 1. On the right side, any point  $x > 1$  is mapped in a point  $f(x) \in (0, 1)$  in one iteration. Thus the range of the map is  $(-\infty, 1]$ , and divergence cannot occur.

To investigate the dynamic properties we can use the first return map  $F_r(x)$  in the interval  $[0, 1]$  on the right side. It is plain that for  $\xi_1 \leq x < 1$ , where  $\xi_1 = O_R^{-1}$ , the definition is  $F_r(x) = f_R(x)$  (in particular  $F_r(\xi_1) = f_R(\xi_1) = 0$ ). While as  $x$  decreases from  $\xi_1$  the map  $F_r(x)$  is defined by the branches  $F_{RL^n}(x)$  for any  $n \geq 1$ . In fact, considering a point on the left side of  $\xi_1$  the first return map is defined by  $F_r(x) = F_{RL}(x) = f_L \circ f_R(x)$  for  $\xi_2 \leq x < \xi_1$  where  $\xi_2 = f_R^{-1} \circ f_L^{-1}(0)$ , and  $F_r(\xi_2) = F_{RL}(\xi_2) = 0$  (while  $F_{RL}(\xi_1) = 1$ ). Then, considering a point on the left side of  $\xi_2$  the first return map is defined by  $F_r(x) = F_{RL^2}(x) = f_L^2 \circ f_R(x)$  for  $\xi_3 \leq x < \xi_2$  where  $\xi_3 = f_R^{-1} \circ f_L^{-2}(0)$ , and notice that  $F_r(\xi_3) = 0$  while  $F_{RL^2}(\xi_3) = 1$  and so on. It is obvious that the process can continue *ad infinitum*, as all the inverses  $f_L^{-n}(0)$  exist for any  $n \geq 1$ , and thus

$$\xi_{n+1} = f_R^{-1} \circ f_L^{-n}(0) \tag{33}$$

all exist for any  $n \geq 1$ , and the first return map has infinitely many branches, given by

$$F_{RL^n}(x) = f_L^n \circ f_R(x) \tag{34}$$

defined in the intervals  $\xi_{n+1} \leq x < \xi_n$  for any  $n \geq 1$  (and  $F_{RL^n}(\xi_{n+1}) = 0$ , while  $F_{RL^n}(\xi_n) = 1$ ).

We have so proved that the first return map in  $[0, 1]$  is a discontinuous map defined by infinitely many increasing branches as stated in the following proposition.

**PROPOSITION 7.** *Let  $\gamma > 0$ ,  $-1 < b < 0$  and  $0 < a \leq 1$ . The dynamics of map  $f$  can be studied by using the first return map  $F_r(x)$  in the interval  $I = [0, 1]$ .  $F_r(x)$  is a discontinuous map with infinitely many branches defined as follows:*

$$F_r(x) := \begin{cases} f_R(x) & \text{if } \xi_1 \leq x \leq 1 \\ \vdots & \vdots \\ F_{RL^n}(x) = f_L^n \circ f_R(x) & \text{if } \xi_{n+1} \leq x \leq \xi_n, \\ \vdots & \vdots \end{cases} \tag{35}$$

where

$$F_{RL^n}(x) = \frac{a^n b}{x^\gamma} + \frac{1 - a^{n+1}}{1 - a} \tag{36}$$

and the discontinuity points are preimages of the origin given by

$$\xi_1 = O_R^{-1} = (-b)^{1/\gamma} < 1 \tag{37}$$

and, for any  $n \geq 1$ , by

$$\xi_{n+1} = f_R^{-1} \circ f_L^{-n}(0) = \left( \frac{-b}{((a^n - 1)/(a^n(a - 1))) + 1} \right)^{1/\gamma}, \tag{38}$$

which have as limit value, as  $n \rightarrow \infty$ , the point  $x = 0$ . Moreover, for any  $n \geq 1$ ,  $F_{RL^n}(\xi_{n+1}) = 0$  and  $F_{RL^n}(\xi_n) = 1$  hold, while the rightmost branch satisfies  $0 \leq F_r(x) = f_R(x) \leq 1 + b$  for  $\xi_1 \leq x \leq 1$ .

An example of the first return map is shown in Figure 8.

The increasing and concave branches of the first return map different from the rightmost one have range from 0 to 1, thus for any  $n \geq 1$  all the branches  $F_r(x) = F_{RL^n}(x)$  exist and intersect the diagonal in repelling fixed points  $x_{RL^n}$  which have  $x = 0$  as limit point as  $n \rightarrow \infty$ . It is easy to see that all these repelling fixed points of  $F_r(x)$ , which represent the basic cycles with symbolic sequence  $RL^n$ , are homoclinic on both sides. From the definition of the first return map  $F_r(x)$  a few properties are immediate, and stated in the following proposition.

**PROPOSITION 8.** Let  $\gamma > 0$ ,  $-1 < b < 0$  and  $0 < a \leq 1$ .

(j.1) Each component  $F_{RL^n}(x)$  of the first return map  $F_r$  is a continuous, increasing and concave function (for  $n = 0$ ,  $F_R(x) = f_R(x)$ ), and the same properties hold for any composition.

(j.2) The composite functions defining a  $k$ -iterate of map  $f$  may undergo either a BCB or a smooth bifurcation related to the eigenvalue  $+1$ .

(j.3) The itinerary of any point for the map  $f$  consists of sequences associated with the syllables  $RL^n$ ,  $n \geq 1$ , related to the branches  $F_{RL^n}(x)$  defining the first return map  $F_r(x)$ , and of syllables  $R^m$ ,  $m \geq 1$ , related to the rightmost branch where  $F_r$  is defined via  $f_R(x)$ .

(j.4) The basic cycles with symbolic sequence  $RL^n$  exist for any  $n \geq 1$  (related to fixed points  $x_{RL^n}$  of  $F_r$  belonging to the branches  $F_{RL^n}(x)$ ) and all are homoclinic on both sides.

Thus, in this range chaotic dynamics always occur. However, as we have shown in Proposition 6, for any fixed value of  $a$ , as  $b$  increases from  $-1$  to  $0$ , the rightmost branch  $f_R(1) = 1 + b$  increases from  $0$  to  $1$ , and in this range of values for  $b$ , attracting cycles may also exist, in particular, for any  $n > 1$  the basic cycles having symbolic sequence  $R^nL$ . That

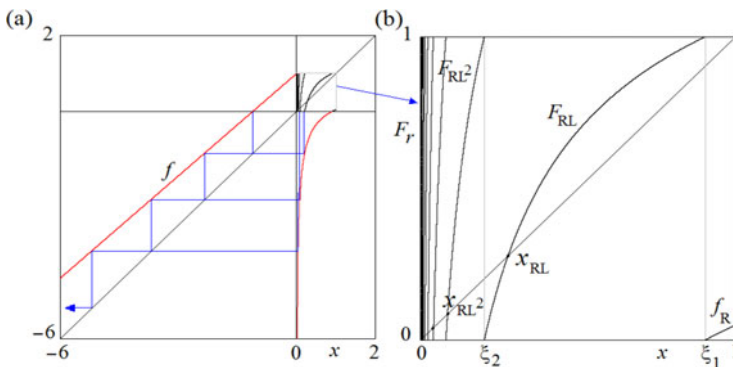


Figure 8. In (a) map  $f$  at  $\gamma = 0.5$ ,  $a = 0.9$ ,  $b = -0.95$ , and its first return map  $F_r(x)$  in  $[0, 1]$  is also shown. In (b) map  $F_r(x)$  is enlarged.

is, even if all the fixed points  $x_{RL^k}$  of  $F_r$  exist and are repelling, for the basic cycles  $R^k\mathcal{L}$  it is also possible to cross fold bifurcation curves, leading to periodicity regions of attracting cycles with the same symbolic sequence  $R^k\mathcal{L}$ , as we can see in Figure 7. In fact, BCBs of attracting cycles may occur, as considered in the next subsection.

4.1.1 BCB of cycles of  $f$

Considering the example shown in Figure 8, we can argue as in Proposition 6. That is, keeping constant the value of the parameter  $a$ , increasing the parameter  $b$  also the value  $F_r(1) = f_R(1) = 1 + b$  increases and the fold bifurcation value  $b(\Phi_R)$  is approached, as shown in Figure 9(b). This implies that the number of right preimages of the discontinuity point  $\xi_1$ , that is, the points  $f_R^{-k}(\xi_1)$ ,  $k \geq 1$ , must increase, being infinitely many when  $b = b(\Phi_R)$ , having as limit point the tangency point  $x_R^*$  in (14). There are no such preimages at small values of  $b$ , as in Figure 8, and the first occurrence ( $k = 1$ ) is shown in Figure 9(a), where it can be seen that  $f_R^{-1}(\xi_1) = 1$ , that is,  $f_R(1) = \xi_1$ , and the BCB value of the 3-cycle  $RL^2$  is reached.

Since  $F_{RL}(\xi_1) = 1$ , this also means that the first return map  $F_r(x)$  has a 2-cycle with periodic points  $\{1, \xi_1\}$  and also that the second iterate of  $F_r(x)$  must have a fixed point in  $x = 1$ , as  $F_{RL} \circ f_R(1) = 1$ . This implies that the rightmost branch of the function  $F_r^2(x)$ , which is given by the function  $F_{RL} \circ f_R(x)$ , takes values from 0 to 1, as shown by an arc in Figure 10(a). Clearly this corresponds to the BCB of a 3-cycle, i.e. the collision of periodic points of a 3-cycle with symbolic sequence  $R^2\mathcal{L}$  with  $x = 0$  and with  $x = 1$ .

As the rightmost branch of the function  $F_{RL} \circ f_R(x)$  intersects the diagonal in two fixed points ( $x_{R\mathcal{L}}$  repelling and  $x_{R\mathcal{L}}^s$  attracting), we can state that an attracting 3-cycle undergoes its BCB, while a repelling 3-cycle persists as  $b$  increases. This also means that at a smaller value of the parameter  $b$  a fold bifurcation of the function  $F_{RL} \circ f_R(x)$  must have been occurred, leading to the appearance of the pair of 3-cycles, as shown by an arc in Figure 10 (b). At the fold bifurcation the function  $F_{RL} \circ f_R(x)$  is tangent to the diagonal in one fixed point  $x_{R\mathcal{L}}^*$  (merging of the repelling  $x_{R\mathcal{L}}$  and attracting  $x_{R\mathcal{L}}^s$  fixed points).

As stated in Proposition 6, as  $b$  increases, all the values  $f_R^k(1) = \xi_1$  must occur, at the BCB curves  $B_{LR^{k+1}}$ , which means that the first return map  $F_r(x)$  has a  $(k + 1)$ -cycle ( $k$  applications of  $f_R$  followed by one application of  $F_{RL}$ ) with periodic points  $\{1, f_R(1), \dots, f_R^k(1) = \xi_1\}$  and also that the  $(k + 1)$ -th iterate of  $F_r(x)$  must have a fixed

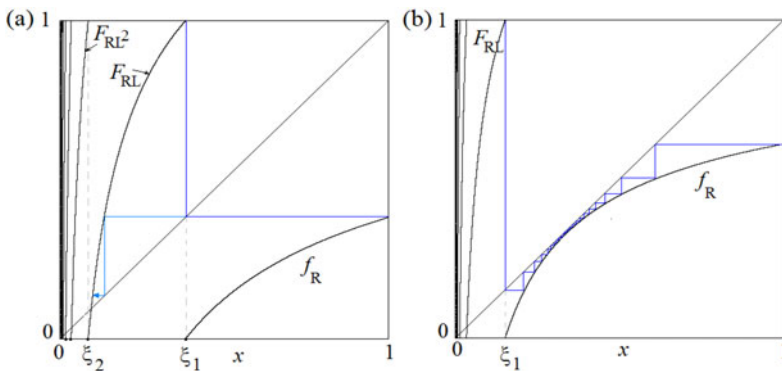


Figure 9. First return map  $F_r(x)$  at  $\gamma = 0.5$ ,  $a = 0.9$ . In (a)  $b = -0.6181$ , BCB of  $LR^2$ . In (b)  $b = -0.39$ , close to the fold bifurcation of  $f_R(x)$ .

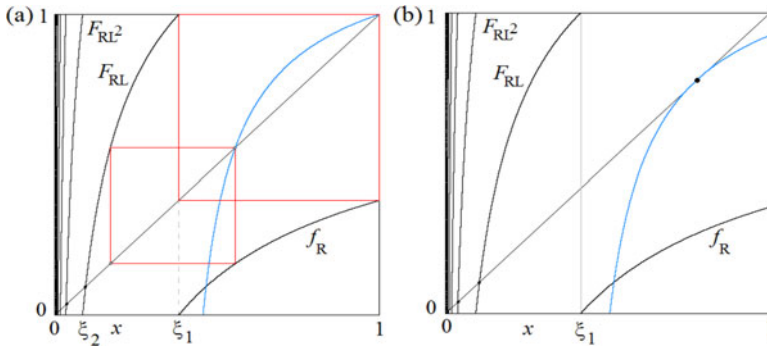


Figure 10. First return map  $F_r(x)$  at  $\gamma = 0.5$ ,  $a = 0.9$ . In (a)  $b = -0.6181$ , BCB of  $LR^2$ . In (b)  $b = -0.645$  fold bifurcation of  $LR^2$ . The added arc is the rightmost branch of the second iterate  $F_r^2(x)$ .

point in  $x = 1$ , as  $F_{RL} \circ f_R^k(1) = 1$ . This implies that the rightmost branch of the function  $F_{RL} \circ f_R^k(x)$  takes values from 0 to 1. Clearly, this corresponds to the BCB of a  $(k + 2)$ -cycle of  $f$  with symbolic sequence  $R^{k+1}L$ , at which the merging of periodic points with  $x = 0$  and with  $x = 1$  occurs.

It is possible that such BCBs of basic cycles always occur with an attracting cycle, for any  $k \geq 1$ , and thus that all these BCBs occur after a value of  $b$  at which a fold bifurcation of a  $(k + 1)$ -cycle of the first return map  $F_r(x)$  (a  $(k + 2)$ -cycle of  $f$ ) takes place, leading to the appearance of a pair of cycles with the same symbolic sequence, one attracting and the other repelling.

Regarding the basic cycles, we can give sufficient conditions to have the BCB occurring with an attracting cycle (and thus, increasing  $b$ , the BCB occurs after the fold bifurcation). In fact, at the BCB of a  $(k + 2)$ -cycle of  $f$  with symbolic sequence  $R^{k+1}L$  we have the periodic points  $\{1 = F_{RL}(\xi_1), f_R(1), \dots, f_R^k(1) = \xi_1\}$  so that in the  $k$  points belonging to the branch  $f_R$  the slope is smaller than 1, and it is

$$F'_{RL}(\xi_1) = a\gamma(-b)^{-1/\gamma}$$

thus a sufficient condition to have an attracting cycle undergoing BCB is given in the following proposition.

**PROPOSITION 9.** *Let  $a > 0$ ,  $\gamma > 0$  and denote by  $b(B_{LR^n})$  the value of the parameter  $b$  at which the BCB of  $LR^n$ ,  $B_{LR^n}$ , occurs. If*

$$b(B_{LR^n}) < -(a\gamma)^\gamma$$

*then the BCB involves an attracting cycle.*

In general, we have seen that for a basic cycle  $R^nL$  a BCB occurs when  $f_R^n(1) = 0$  and it may be in pair with a fold bifurcation, which occurs when two fixed points are merging in a point  $x^* \in (0, 1)$  which is a solution of the equation

$$f_L \circ f_R^n(x) = x$$

that can also be rewritten as follows:

$$f_R^n(x) = \frac{1}{a}(x - 1). \tag{39}$$



This equation shows that, differently from the BCB of the basic cycles  $LR^n$ , and differently from the fold bifurcation of the fixed points of  $f_R(x)$  (which do not depend on  $a$ ), the fold bifurcation curves also depend on the value of the parameter  $a$ . The fold bifurcation of a basic cycle  $LR^n$  happens when the iterate  $f_R^n(x)$  (function with increasing and concave branches, which depends only on  $b$ ) becomes tangent in a point  $x^* \in (0, 1)$  to the straight line of equation  $(x - 1)/a$  (connecting the points  $(0, -(1/a))$  and  $(1, 0)$  of the plane  $(x, x') = (x, f(x))$ , and depending only on  $a$ ). For example, the case shown in Figure 10(b) corresponds also to the one in Figure 11, where the function  $f_R^2(x)$  is tangent to the straight line  $(x - 1)/0.9$  exactly in the two merging fixed points of the function  $F_{RL} \circ f_R(x)$  (rightmost branch of  $F_r^2(x)$ ) in Figure 10(b) (corresponding to the rightmost fixed point of the 3-cycles for the map  $f$ ).

This also explains why at small values of the parameter  $a$  it is more likely to have fold bifurcation curves. In fact, when  $a$  is small the slope  $1/a$  becomes larger, and it is more likely to have the branches of the functions  $f_R^n(x)$  which become tangent to that line in the required interval, for many different values of  $n$ . When  $a$  is larger, the tangency can be virtual, it does not take place in the interval  $(0, 1)$  so that a BCB of basic cycles can occur without a ‘previous’ fold bifurcation, and is related to a repelling cycle.

So, it can be expected that BCBs may occur without a previous fold bifurcation, *also for not basic cycles*. An example is given in Figure 12. In that figure, the parameter  $b$  is such that

$$f_R(1) = \xi_2 \tag{40}$$

and considering that  $F_{RL^2}(\xi_2) = f_L^2 \circ f_R(\xi_2) = f_L(0) = 1$ , by applying  $F_{RL^2}(x)$  to both sides in (40) we obtain

$$F_{RL^2} \circ f_R(1) = f_L^2 \circ f_R^2(1) = 1$$

which means that a BCB of a cycle with symbolic sequence  $R^2L^2$  occurs. It is also a 2-cycle of the first return map  $F_r(x)$  involving the rightmost branch  $f_R(x)$  and the branch  $F_{RL^2}(x)$ , and it can be seen as a fixed point of the rightmost branch of  $F_r^2(x)$ , which is now

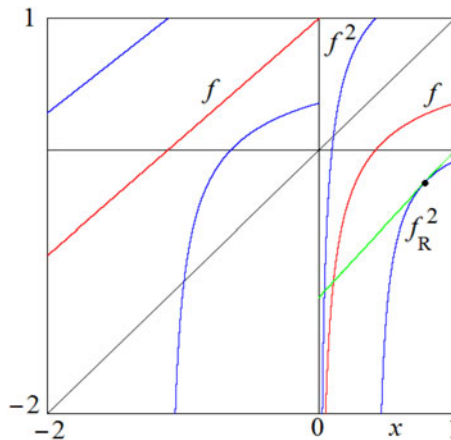


Figure 11. Map  $f(x)$  at  $\gamma = 0.5$ ,  $a = 0.9$ ,  $b = -0.645$ , which corresponds to the fold bifurcation of  $LR^2$ . The second iterate,  $f^2(x)$ , and the rightmost branch is tangent to the straight line in (39).



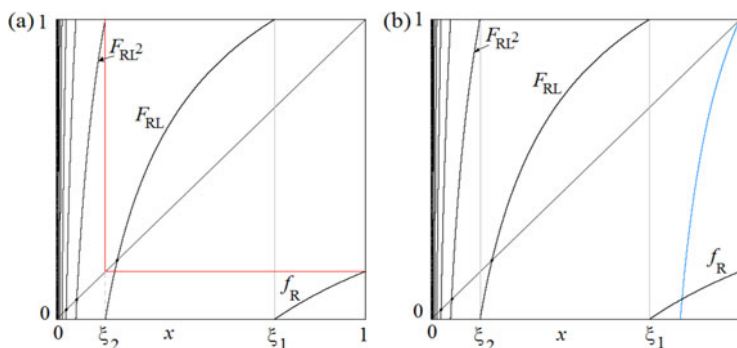


Figure 12. First return map  $F_r(x)$  at  $\gamma = 0.5, a = 0.9, b = -0.841$ , BCB of the unstable cycle  $R^2L^2$ . In (b) the arc is the rightmost branch of the second iterate  $F_r^2(x)$ .

given by the function  $F_{RL^2} \circ f_R(x)$ , which takes values from 0 to 1, as shown by an arc in Figure 12(b). The BCB of the 4-cycle of  $f$  occurs without a companion attracting 4-cycle. This can be deduced from the slope of the function  $F_r^2(x)$  in the point  $x = 1$ , that is the slope of the function  $F_{RL^2} \circ f_R(x)$  in the point  $x = 1$ . It is larger than 1, so that for larger values of  $b$  the single 4-cycle appears repelling and it will persist repelling for any larger value of  $b$  in this parameter range.

By construction of the first return map  $F_r(x)$  the discontinuity points of  $F_r(x)$  occur at the points  $\xi_j, j \geq 1$  which are preimages of the origin (as given in (37) and in (38)). Moreover, for any  $j \geq 1$  it is

$$F_{RL^j}(\xi_j) = 1. \tag{41}$$

From this we have seen that whenever the point  $F_r(1) = f_R(1)$  merges with a preimage of the origin of any rank, say  $\xi_j^{-k}$ , for  $k \geq 0$  ( $k = 0$  leads to  $\xi_j$ ) so that

$$f_R(1) = \xi_j^{-k} \tag{42}$$

then a BCB of a cycle occurs. In fact, if  $k = 0$  we have

$$F_{RL^j} \circ f_R(1) = 1, \tag{43}$$

leading to a BCB of the cycle of  $f$  with symbolic sequence  $R^2L^j$  (the case corresponding to  $j = 2$  has been shown above).

For  $k \geq 1$  let

$$\xi_j^{-k} = F_r^{-k}(\xi_j) = F_{RL^{n_k}}^{-1} \circ \dots \circ F_{RL^{n_1}}^{-1}(\xi_j) \tag{44}$$

where  $F_{RL^{n_i}}^{-1}(\xi_j)$  represent the involved branches of the first return map, with  $n_i \geq 0$  for  $i = 1, \dots, k$  (for  $n_i = 0$  it holds  $F_{RL^{n_i}}^{-1}(x) = f_R^{-1}(x)$ , i.e. the inverse of the rightmost branch of  $F_r$ ). From

$$f_R(1) = F_r^{-k}(\xi_j) = F_{RL^{n_k}}^{-1} \circ \dots \circ F_{RL^{n_1}}^{-1}(\xi_j)$$

we can write

$$F_{RL^{n_1}} \circ \dots \circ F_{RL^{n_k}} \circ f_R(1) = \xi_j$$

and thus, by applying  $F_{RL^j}$  on both sides, we have

$$F_{RL^j} \circ F_{RL^{n_1}} \circ \dots \circ F_{RL^{n_k}} \circ f_R(1) = 1 \quad (45)$$

representing the BCB of a cycle of the first return map  $F_r$  (of period  $(k + 2)$ ), and a cycle of  $f$  with symbolic sequence

$$RRL^{n_k} \dots RL^{n_1} RL^j. \quad (46)$$

We remark that for the first return map the BCB in (42) also corresponds to

$$F_r^{k+1}(1) = \xi_j$$

(that is, the trajectory of  $x = 1$  for the first return map  $F_r$  is mapped to a discontinuity point of  $F_r$ ), so that by using  $F_{RL^j}(\xi_j) = 1$  and  $F_{RL^{j-1}}(\xi_j) = 0$ , it can also be written as

$$F_{RL^j} \circ F_r^{k+1}(1) = 1 \quad (47)$$

or, equivalently,

$$F_{RL^{j-1}} \circ F_r^{k+1}(1) = 0. \quad (48)$$

Moreover, from the above conditions we can notice that at each BCB the properties of the iterate of order  $(k + 2)$  of the first return map are similar (with obvious changes) to those commented above for the BCB of the basic cycle  $R^2L$  and for the BCB of the cycle  $R^2L^2$  of  $f$  as fixed points of  $F_r$ . That is, a suitable iterate of the first return map,  $F_r^{k+2}(x)$ , has the rightmost branch which is increasing from 0 to 1. Then what matters is the first derivative of that rightmost branch of the function  $F_r^{k+2}$  in the point  $x = 1$ . Recall that all the composite functions consist of branches which are monotone increasing and concave, so that the first derivative exists and is necessarily positive and decreasing. So, at a BCB value, considering the first derivative  $D$  of the function  $F_{RL^j} \circ F_{RL^{n_1}} \circ \dots \circ F_{RL^{n_k}} \circ f_R(x)$  in the point  $x = 1$ :

$$D = \frac{d}{dx} (F_{RL^j} \circ F_{RL^{n_1}} \circ \dots \circ F_{RL^{n_k}} \circ f_R)(x)|_{x=1} \quad (49)$$

we can state that

(i.1) if  $D \geq 1$  then the crossing of the BCB curve increasing  $b$  leads to the appearance of a repelling cycle (having the symbolic sequence given in (46));

(i.2) if  $D < 1$  then the crossing of the BCB curve increasing  $b$  leads to the disappearance of an attracting cycle (having the symbolic sequence given in (46)), leaving a repelling cycle with the same symbolic sequence (which means that at smaller values of  $b$  a fold bifurcation of cycles having the same symbolic sequence must occur, leading to their existence).

When  $D < 1$ , the suitable iterate  $F_r^{k+2}(x)$  of the first return map has the point  $x = 1$  which is attracting from its left side, with immediate basin  $(x_\sigma, 1]$  where  $\sigma = RRL^{n_k} \dots RL^{n_1} RL^j$ , and  $x_\sigma$  is homoclinic on its left side, while all the other repelling fixed points are homoclinic on both sides. Thus, almost all the points are converging to 1, that is, all the points except for those of a chaotic repeller in  $[0, x_\sigma]$  for the first return map  $F_r$ , in  $(-\infty, x_\sigma]$  for the map  $f$ .

Noticing that the function  $F_{RL^j} \circ F_{RL^{n_1}} \circ \dots \circ F_{RL^{n_k}} \circ f_R(x)$  is monotone increasing and concave, so that its first derivative is positive and decreasing, we can conclude that on any BCB curve (the existence of infinitely many of them will be proved below), a particular codimension-two point may exist (related to the value  $D = 1$ ), separating the curve in two different parts, associated with different dynamic properties, as for the BCB curves  $B_{RL^n}$  of the basic cycles considered in Section 3. That is, crossing a BCB curve in a point above ( $D > 1$ ) or at ( $D = 1$ ) its codimension-two point, a repelling cycle is created which persists for any larger value of  $b$ , while crossing a BCB curve below its codimension-two point ( $D < 1$ ) an attracting cycle (born by fold bifurcation at a smaller value of  $b$ ) disappears, leaving the repelling one for any larger value of  $b$ . We can so state the following proposition.

**PROPOSITION 10.** *Let  $a > 0$ ,  $\gamma > 0$  and  $-1 \leq b < b(\Phi_R) = -(1/\gamma)(\gamma/(\gamma + 1))^{\gamma+1}$ . When  $f_R(1)$  merges with the preimage of a discontinuity point of the first return map  $F_r$ , say*

$$f_R^m(1) = F_r^{-k}(\xi_j) = F_{RL^{n_k}}^{-1} \circ \dots \circ F_{RL^{n_1}}^{-1}(\xi_j)$$

where  $m \geq 1$ ,  $n_i \geq 0$  for  $i = 1, \dots, k$  with  $\sum_i n_i = k$  ( $F_{RL^0}^{-1} = f_R^{-1}$  for  $n_i = 0$ ) then the BCB of a cycle of period  $(m + 1 + k)$  of the first return map  $F_r$  occurs, corresponding to the BCB of a cycle of  $f$  with symbolic sequence

$$R^m RL^{n_k} \dots RL^{n_1} RL^j. \tag{50}$$

Let

$$D = \frac{d}{dx} (F_{RL^j} \circ F_{RL^{n_1}} \circ \dots \circ F_{RL^{n_k}} \circ f_R^m)(x)|_{x=1} \tag{51}$$

if  $D \geq 1$  then the colliding cycle appears repelling, and persists repelling for larger values of  $b$  (without an attracting cycle with the same symbolic sequence);

if  $D < 1$  then the colliding cycle is attracting, and disappears for larger values of  $b$ , while a repelling cycle with the same symbolic sequence, born by fold bifurcation at a smaller value of  $b$ , persists for larger values of  $b$ .

At small values of the parameter  $a$ , by increasing  $b$  more regions of attracting cycles can be observed. Differently, when  $a$  approaches 1 the repelling cycles become dominant.

In Figure 13(a) the complete range of  $b$  values from  $-1$  to the value  $b(\Phi_R)$ , related to the appearance of the attracting fixed point by fold bifurcation in  $f_R(x)$ , is shown at

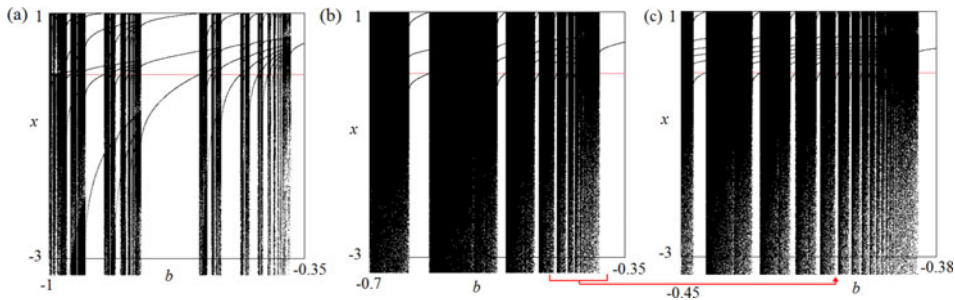


Figure 13. One-dimensional bifurcation diagrams of  $x$  as a function of  $b$ , at  $\gamma = 0.5$ . In (a)  $a = 0.2$  is fixed. In (b)  $a = 0.9$  is fixed. In (c) an enlarged part of (b) is shown.

Downloaded by [93.150.144.95] at 06:43 19 June 2015

$a = 0.2$ , and several attracting cycles can be observed. While at  $a = 0.9$  in Figure 13(b) it is shown only the range of  $b$  from the value  $-0.7$  (as before no attracting cycle can be detected numerically), an enlargement in Figure 13(c) shows that only the basic cycles are observable as attracting.

It is clear that the preimages of the discontinuity points in the first return map are infinitely many, their limit points include all the existing repelling cycles (all SBR). For example at the parameter value used in Figure 9(a) we can see that the value  $f_R(1)$  has already crossed infinitely many preimages, and infinitely many BCB values have already been crossed. In fact, in Figure 9(a) a sequence of preimages of  $\xi_1$ ,  $F_{RL}^{-k}(\xi_1)$  is accumulating as  $k \rightarrow \infty$  to the repelling fixed point  $x_{RL}$  so that all the BCBs having equation

$$f_R(1) = F_{RL}^{-k}(\xi_1) \tag{52}$$

that is

$$F_{RL}^{k+1} \circ f_R(1) = 1 \tag{53}$$

associated with cycles of  $f$  having symbolic sequence  $R(RL)^{k+1}$  must have been occurred. This symbolic sequence can also be written as  $R^2L(RL)^k$  or, equivalently, as  $LR^2(LR)^k$  for any  $k \geq 1$ , and leads to a family of BCB curves which are issuing from the first codimension-two point intersection between the BCB curve of the cycles LR and the smooth fold bifurcation curve of the cycle  $LR^2$ , see the enlargement in Figure 14(a).

Clearly, the value of  $a$  in Figure 9(a) is quite large, and the crossing of the BCB curves is mainly associated with the appearance of repelling cycles, while at the value of  $a$  used in Figure 14(a) the crossing of at least some of the BCB curves issuing from the codimension-two point is associated with attracting cycles (having the same symbolic sequence), thus they occur after the crossing of related fold bifurcation curves. Two examples are illustrated in Figure 15, BCB of the 5-cycle  $LR^2LR$  and of the 7-cycle  $LR^2(LR)^2$ .

It is easy to see how many different families of BCB curves exist. For example sequences of preimages of  $\xi_1$ , can be considered accumulating also to all the other repelling fixed points  $x_{RL^j}$  that is, for any  $j > 1$ ,  $F_{RL^j}^{-k}(\xi_1)$  are accumulating as  $k \rightarrow \infty$  to the repelling fixed point  $x_{RL^j}$  thus all the BCB curves having equation

$$f_R(1) = F_{RL^j}^{-k}(\xi_1) \tag{54}$$

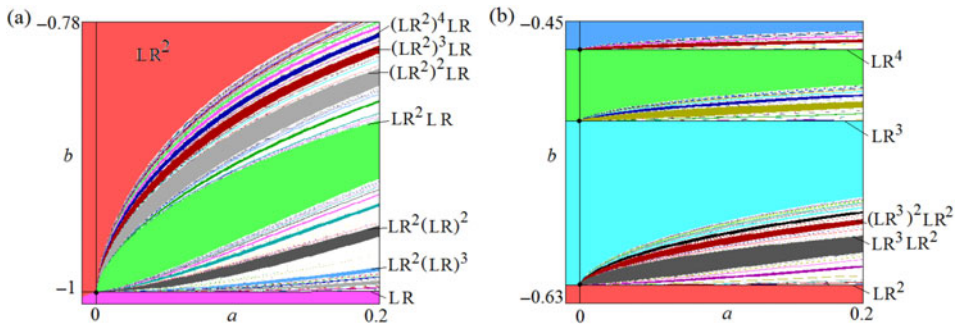


Figure 14. Enlarged parts of organizing centres in Figure 7(b) ( $\gamma = 0.5$ ).

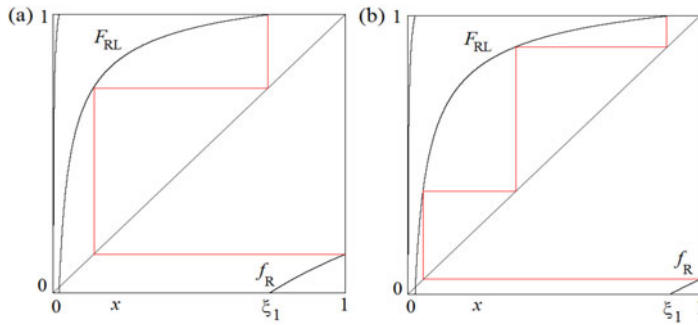


Figure 15. Map  $F_r(x)$  at  $\gamma = 0.5$ ,  $a = 0.2$ . In (a)  $b = -0.861$ , BCB of the 5-cycle  $LR^2LR$  of  $f(x)$ . In (b)  $b = -0.947$  BCB of the 7-cycle  $LR^2(LR)^2$  of  $f(x)$ .

that is

$$F_{RL} \circ F_{RL}^k \circ f_R(1) = 1 \tag{55}$$

must have been crossed, associated with cycles of  $f$  having symbolic sequence  $R(RL^j)^k RL$  for any  $k \geq 1$  and any  $j > 1$ .

Also the preimages of  $\xi_2$  can be considered, for example  $F_{RL}^{-k}(\xi_2)$  which are accumulating as  $k \rightarrow \infty$  to the repelling fixed point  $x_{RL}$ , or  $F_{RL^2}^{-k}(\xi_2)$  which are accumulating as  $k \rightarrow \infty$  to the repelling fixed point  $x_{RL^2}$ , leading to the BCB curves of equations

$$\begin{aligned} f_R(1) &= F_{RL}^{-k}(\xi_2) \\ F_{RL^2} \circ F_{RL}^k \circ f_R(1) &= 1 \end{aligned} \tag{56}$$

and

$$\begin{aligned} f_R(1) &= F_{RL^2}^{-k}(\xi_2) \\ F_{RL^2}^{k+1} \circ f_R(1) &= 1 \end{aligned} \tag{57}$$

associated with cycles of  $f$  having symbolic sequence  $R(RL)^k RL^2$  for any  $k \geq 1$  and  $R(RL^2)^{k+1}$  for any  $k \geq 1$ . In general for any  $\xi_n$  we have

$$\begin{aligned} f_R(1) &= F_{RL^{n-1}}^{-k}(\xi_n) \\ F_{RL^n} \circ F_{RL^{n-1}}^k \circ f_R(1) &= 1 \end{aligned} \tag{58}$$

and

$$\begin{aligned} f_R(1) &= F_{RL^n}^{-k}(\xi_n) \\ F_{RL^n}^{k+1} \circ f_R(1) &= 1 \end{aligned} \tag{59}$$

for any  $n \geq 1$  associated with cycles of  $f$  having symbolic sequence  $R(RL^{n-1})^k RL^n$  for any  $k \geq 1$  and  $R(RL^n)^{k+1}$  for any  $k \geq 1$ .

Let us also show the BCBs which are associated with other cycles are clearly visible in Figure 14(a) of symbolic sequence  $(LR^2)^k LR$  for any  $k \geq 1$ . They obviously involve the preimages  $(f_R^{-1} \circ F_{RL}^{-1})^k(\xi_1)$  so that we have

$$\begin{aligned} (F_{RL} \circ f_R)^k(1) &= \xi_1 \\ F_{RL} \circ (F_{RL} \circ f_R)^k(1) &= 1 \end{aligned} \tag{60}$$

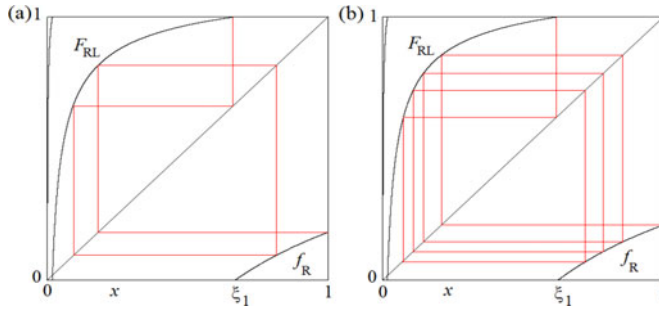


Figure 16. Map  $F_r(x)$  at  $\gamma = 0.5$ ,  $a = 0.2$ . In (a)  $b = -0.818$ , BCB of the 8-cycle  $(LR^2)^2LR$  of  $f(x)$ . In (b)  $b = -0.79$ , BCB of the 14-cycle  $(LR^2)^4LR$  of  $f(x)$ .

leading to BCB of cycles with symbolic sequence  $RL(RLR)^k$  that is, equivalently,  $(LR^2)^kLR$ . Two examples related to  $k = 2$  and  $k = 4$  are illustrated in Figure 16, BCB of the 8-cycle  $(LR^2)^2LR$  and of the 14-cycle  $(LR^2)^4LR$ .

From Figure 14(a),(b) we can see that all the BCB curves and fold bifurcation curves are issuing from particular codimension-two points which are the intersection points of the BCB of the basic cycles  $LR^n$  with the fold bifurcation curves of basic cycles  $LR^{n+1}$ . Such points play the role of organizing centres, or big bang bifurcation points, and belong to the line  $a = 0$  which also is a particular curve, as it can be considered the BCB curve of cycles with the point at infinity,  $-\infty$ , and especially for map  $f$  it represents the transition non-invertible/invertible.

The sequence of bifurcation curves issuing between the periodicity regions of the cycles  $LR$  and  $LR^2$  shown in Figure 14(a) is repeated with obvious changes between the BCB curves of cycles  $LR^n$  and  $LR^{n+1}$  for any  $n > 1$ , and clearly, as we have shown above, the limit set of the BCB curves of the basic cycles is the fold bifurcation curve of the fixed points of  $f_R(x)$ .

In Figure 14(b) we can see that several families of BCB curves occur after a related fold bifurcation. For example, a family of BCB curves exists, accumulating to the fold bifurcation curve of  $LR^3$ ,  $\Phi_{LR^3}$ , satisfying the following equation, for all  $k \geq 1$  :

$$f_R(F_{RL} \circ f_R^2)^k(1) = \xi_1$$

that is

$$F_{RL} \circ f_R(F_{RL} \circ f_R^2)^k(1) = 1$$

related to cycles having the symbolic sequences  $(LR^3)^kLR^2$ . In Figure 17(a) we illustrate the BCB of the 7-cycle  $LR^3LR^2$  ( $k = 1$ ) and in Figure 17(b) that of the 11-cycle  $(LR^3)^2LR^2$  ( $k = 2$ ).

#### 4.1.2 Homoclinic bifurcations

As we have seen above, whenever the point  $f_R(1)$  merges with the preimage of a discontinuity point of the first return map  $F_r$ , then a BCB occurs. Similarly we have that whenever the point  $f_R(1)$  is preperiodic to a cycle, then another homoclinic bifurcation of the cycle occurs. This and other properties are given in the following proposition.

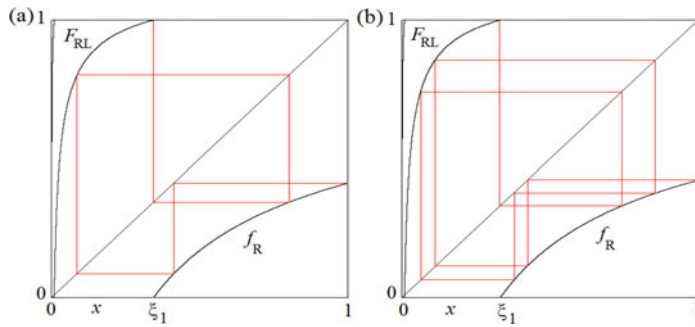


Figure 17. Map  $F_r(x)$  at  $\gamma = 0.5$ ,  $a = 0.2$ . In (a)  $b = -0.587$ , BCB of the 7-cycle  $LR^3LR^2$  of  $f(x)$ . In (b)  $b = -0.5762$  BCB of the 11-cycle  $(LR^3)^2LR^2$  of  $f(x)$ .

PROPOSITION 11. Let  $\gamma > 0$ ,  $0 < a \leq 1$  and  $-1 < b < 0$ .

- (1) If the point  $f_R(1)$  merges with the preimage of a repelling periodic point of the first return map  $F_r$ , then a homoclinic bifurcation of the cycle occurs.
- (2) All the repelling cycles of  $f$  are homoclinic at least on one side.
- (3) Each homoclinic bifurcation curve is a limit set of BCB curves.
- (4) Each BCB curve is a limit set of other BCB curves.
- (5) The map  $f$  always has an unbounded chaotic set in  $(-\infty, 1]$ .
- (6) The map  $f$  cannot have divergent trajectories.

Proof.

- (1) Assume that the point  $f_R(1)$  merges with the preimage of a repelling periodic point  $x^*$  of the first return map  $F_r$ , say

$$f_R^m(1) = F_r^{-k}(x^*) = F_{RL}^{-1} \circ \dots \circ F_{RL}^{-1}(x^*), \tag{61}$$

then a homoclinic bifurcation of the cycle occurs. In fact, it holds  $F_r^k \circ f_R^m(1) = x^*$  at the bifurcation value, and at a smaller value of  $b$  (before the bifurcation) it must be  $F_r^k \circ f_R^m(1) < x^*$  while at a larger value of  $b$  (after the bifurcation) it must be  $F_r^k \circ f_R^m(1) > x^*$ . Thus after the bifurcation the periodic point  $x^*$  has preimages starting with  $f_R^{-1}(x^*)$  which did not exist before the bifurcation. This leads to an explosion of homoclinic orbits of the same cycle which did not exist before the bifurcation, proving that it is a new homoclinic bifurcation.

- (2) To show that all the repelling cycles are homoclinic at least on the left side, consider a repelling  $n$ -cycle of the first return map  $F_r$  and a fixed point  $z^*$  of the map  $F_r^n$  belonging to the cycle of  $F_r$  and to a branch  $F_\sigma$  of the map  $F_r^n$ . Then preimages on the left side of  $z^*$  exist which are accumulating to all the repelling fixed points of the first return map  $F_r$  (having as limit point  $x = 0$ ), and each preimage on the left side of  $z^*$  has a preimage on the branch  $F_\sigma$  thus leading to an homoclinic orbit of  $z^*$ . With a similar argument we can say that except for the repelling cycle which exists with a companion attracting cycle, all the other repelling cycles are homoclinic on both sides.
- (3) To show that homoclinic bifurcation curves are limit sets of BCB curves, consider the homoclinic bifurcation value at which  $f_R^m(1) = F_r^{-k}(x^*)$  occurs, then



$F_r^k \circ f_R^m(1) = x^*$ , which also implies that at a smaller value of  $b$  it is  $F_r^k \circ f_R^m(1) < x^*$  while at a larger value of  $b$  it is  $F_r^k \circ f_R^m(1) > x^*$ . This means that after the bifurcation preimages of the discontinuity points, which did not exist before, are accumulating to  $x^*$  from above, thus the homoclinic bifurcation value is a limit set of BCB values.

- (4) To show that BCB curves are limit sets of other BCB curves, consider a bifurcation value related to an  $n$ -cycle of the first return map  $F_r$ , then the rightmost branch of the map  $F_r^n$  ranges from 0 to 1 and at the bifurcation value either a repelling fixed point merges with  $x = 1$ ,  $x_\sigma = 1$ , or an attracting one,  $x_\sigma^s = 1$ . In the first case, for a larger value of  $b$ , after the bifurcation, a repelling cycle appears (which persists for larger values of  $b$ ) leading to a new fixed point  $x_\sigma < 1$  in the map  $F_r^n$  and preimages of the discontinuity points of the first return map  $F_r$ , which did not exist before, are accumulating to  $x_\sigma$  from above, thus the BCB value is a limit set of other BCB values. Similarly in the second case, when  $x_\sigma^s = 1$ , for a larger value of  $b$ , after the bifurcation, the repelling cycle having the same symbolic sequence of the attracting cycle which disappeared is left (and it persists for larger values of  $b$ ). Then after the bifurcation the fixed point  $x_\sigma < 1$  has preimages in the map  $F_r^n$  also on its right side, which did not exist before. Moreover, in the map  $F_r^n$ , preimages of the discontinuity points of the first return map  $F_r$ , which did not exist before, are accumulating to  $x_\sigma$  from above, thus the BCB value is a limit set of other BCB values.
- (5) The property (2) of the first return map  $F_r$  given above (repelling cycles which are homoclinic) proves that the first return map  $F_r$  always has a chaotic set in  $[0, 1]$ , even if there exists an attracting cycle. In terms of the map  $f$ , this means that an unbounded chaotic set in  $(-\infty, 1]$  always exists.
- (6) It is also plain that divergent trajectories cannot exist, as each point in  $[0, 1]$  has the trajectory which returns back in  $[0, 1]$ .  $\square$

In the next section we shall see that in the last range here considered, when a repelling fixed point  $x_L^*$  exists, for  $-1 < b < 0$ , then the chaotic sets, which also always exist, can only be bounded, while a set of points of positive measure exists with divergent trajectories.

#### 4.2 Range BII ( $a > 1$ , $-1 < b < 0$ ,) : bounded chaotic repellers

The properties of the dynamic behaviours in this range mainly depend on the fact that the slope of the function  $f_L(x)$  is larger than 1, so that the repelling fixed point  $x_L^* = -1/(a-1) < 0$  exists. As in Section 3 let us denote by  $B_\infty$  the set of positive measure of points having divergent trajectories (basin of  $-\infty$ , or set of divergent trajectories). As usual, it is given by all the preimages of any rank of the immediate basin, which is the interval  $(-\infty, x_L^*)$ , so that

$$B_\infty = \bigcup_{k=0}^{\infty} f^{-k}(-\infty, x_L^*). \quad (62)$$

The first preimage of the immediate basin is  $f_R^{-1}((-\infty, x_L^*)) = (0, x_L^{*-1})$  which is the right neighbourhood of the origin bounded by the preimage  $x_L^{*-1} = f_R^{-1}(x_L^*)$ , given by

$$x_L^{*-1} = \left( \frac{b}{x_L^* - 1} \right)^{1/\gamma} = \left( \frac{-b(a-1)}{a} \right)^{1/\gamma},$$



and clearly for  $b > -1$  it is always  $x_L^{*-1} < O_R^{-1}$ . Thus for any  $-1 < b < 0$  an invariant set of bounded dynamics exists in  $(-\infty, 1]$ , which can be of positive measure (and including a chaotic set) or a chaotic set of zero measure. The two different behaviours depend on the existence or non-existence of an attracting cycle, respectively. Moreover, when an attracting cycle exists, a bounded chaotic repeller always exists in the interval  $[x_L^*, 1]$ .

To prove these properties, we still make use of a first return map. In fact, regarding the function on the right side, we recall that in one iteration any point  $x > 1$  is mapped to a point  $f_R(x) \leq 1$ . Thus, even if in  $(0, 1)$  there exist points having divergent trajectories, following the same reasoning as in Section 3, we can still study the dynamics of the map by using the first return map in  $[0, 1]$  but considering only the first return of the points in the interval  $(x_L^{*-1}, 1]$ , as for the remaining points we know that the trajectory never comes back (as the interval  $(0, x_L^{*-1}]$  is mapped in the immediate basin of infinity  $(-\infty, x_L^*]$ ). Clearly, the interval  $(0, x_L^{*-1})$  represents a set of initial conditions having divergent trajectories, and all the points which are mapped in this interval will have divergent trajectories too.

**PROPOSITION 12.** *Let  $\gamma > 0$ ,  $a > 1$  and  $-1 < b < 0$ . The dynamics of map  $f$  can be described by using the first return map  $F_r(x)$  in the interval  $I = [0, 1]$  taken for the points in the interval  $J = (x_L^{*-1}, 1]$ .  $F_r(x)$  is a discontinuous map with infinitely many branches as defined in (35), in which the discontinuity points are accumulating to  $x = x_L^{*-1}$ .*

*Proof.* Starting from the first return of the point  $x = 1$ , as described in the previous section, with the rightmost branch given by  $f_R(x)$ , the infinitely many preimages  $f_L^{-n}(0)$  all exist, and have as limit set the repelling fixed point  $x_L^*$ . Thus the infinitely many preimages  $\xi_j, j \geq 1$ , discontinuity points of  $F_r(x)$ , all exist in the interval  $(x_L^{*-1}, 1]$ , and have  $x_L^{*-1}$  as limit point for  $j \rightarrow \infty$ . □

This also implies the existence of infinitely many repelling (and all homoclinic) fixed points  $x_{RL^n}$  (basic cycles  $RL^n$  of  $f$ ).

An example with a pair of 2-cycles of the first return map is shown in Figure 18(a). In that case, for map  $f$  there exists an attracting 3-cycle  $LR^2$ , and thus also a companion repelling one.

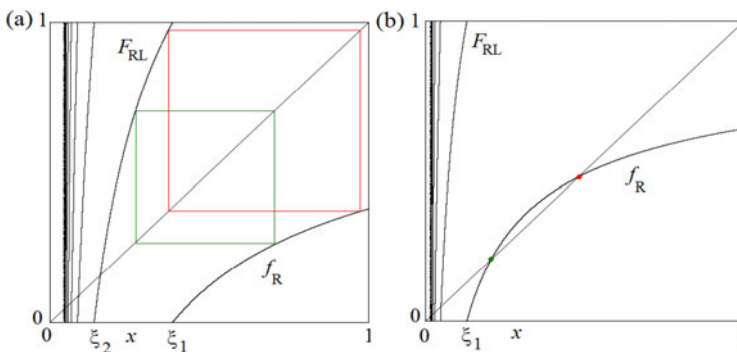


Figure 18. Stable cycles and divergent trajectories at  $\gamma = 0.5$ ,  $a = 1.5$ . In (a)  $b = -0.62$ . In (b)  $b = -0.36$ .

Downloaded by [93.150.144.95] at 06:43 19 June 2015

In general, when an attracting  $(n + 1)$ -cycle  $LR^n$  exists, let  $x_{LR^n}^s$  be the rightmost periodic point of the attracting cycle, and  $x_{LR^n}$  be the rightmost periodic point of the repelling cycle ( $x_{LR^n} < x_{LR^n}^s$ ). The interval  $(x_{LR^n}, 1]$  belongs to the basin of the attracting cycle and the total basin of attraction of the attracting cycle is given by all its preimages of any rank. Such a basin has positive measure, and a fractal structure. In fact, its frontier includes a chaotic repeller  $\Lambda$  which consists of all the repelling cycles, their stable sets and related limit points. There is also another basin of positive measure, that of the divergent trajectories, given by the interval  $(0, x_L^{*-1})$  and all its preimages in the interval  $(x_L^{*-1}, 1]$ , which also has a fractal structure. The frontier between the two basins (both of positive measure) includes all the preimages of the point  $x_L^{*-1}$  (which are dense in a chaotic repeller  $\Lambda$ ).

We can reason in a similar way for any attracting cycle with symbolic sequence  $\sigma$ , denoting  $x_\sigma$  and  $x_\sigma^s$  the two rightmost periodic points of the repelling and attracting cycle, respectively, where  $x_\sigma < x_\sigma^s$ . For the map  $f$  the two basins of the first return map have the same properties and cover the whole real line  $(-\infty, \infty)$ . However, the chaotic repeller of map  $f$  is confined in the interval  $[x_L^*, x_\sigma]$ . In particular it holds for  $\sigma = R$ , when an attracting fixed point of  $f_R(x)$  exists (an example is shown in Figure 18(b)).

The other possible dynamic behaviour mentioned above occurs when the map has no attracting cycle. In such a case, a chaotic repeller  $\Lambda$  exists in the interval  $(x_L^{*-1}, 1]$  which includes all the repelling cycles, their stable sets and related limit points. Taking the preimages by  $F_r(x)$  of the interval  $(0, x_L^{*-1})$  we have that almost all the points of the interval  $(x_L^{*-1}, 1]$  belong to the basin  $B_\infty$ . These preimages have a fractal structure, and are dense in the interval  $(x_L^{*-1}, 1]$ , and the frontier is given by the chaotic repeller  $\Lambda$ . For the map  $f$  this means that a chaotic repeller belongs to  $[x_L^*, 1]$  and all the other points have a divergent trajectory.

We have so proved the following proposition.

**PROPOSITION 13.** *Let  $\gamma > 0$ ,  $a > 1$  and  $-1 < b < 0$ . The dynamics of map  $f$  can be classified as follows:*

- (1) *if  $(a, b)$  does not belong to the stability region of some attracting cycle, almost all the trajectories are divergent, except for a chaotic repeller included in the interval  $[x_L^*, 1]$ ;*
- (2) *if  $(a, b)$  belongs to the stability region of some attracting cycle with symbolic sequence  $\sigma$ , there exist two basins of positive measure. The basin  $B(x_\sigma^s) = \cup_{k=0}^{\infty} f^{-k}(x_\sigma, 1]$  where  $x_\sigma$  and  $x_\sigma^s$  are the two rightmost periodic points of the repelling and attracting cycles, respectively. The basin of divergent trajectories is given by  $B(x_\sigma^s) = \cup_{k=0}^{\infty} f^{-k}(-\infty, x_L^*)$ . The frontier between the two basins belongs to a chaotic repeller included in the interval  $[x_L^*, x_\sigma]$ .*

## 5. Conclusions and outlook

In this work we have further investigated some properties of the discontinuous map given in (2) for the parameter ranges given in (3) when the map has the qualitative shapes shown in Figure 1. In each case the results are obtained making use of the first return map in a suitable interval. A common result to all the three different cases is that any BCB may be related to a codimension-two point due to the contact with a fold bifurcation curve of cycles with the same symbolic sequence. However, the dynamics are different in the different ranges. In Range AII,  $-\infty$  is always an attractor with a basin of attraction  $B_\infty$  of

positive measure. However, for parameters above the curve  $B_f$  (homoclinic bifurcation of the unstable fixed point  $x_f^*$ ) chaotic repeller exists which belongs to the frontier of the basin of attraction  $B_\infty$  and an attracting cycle may also exist. In the Range BI divergence cannot occur, and an unbounded chaotic repeller always exists, while in Range BII we have shown that the system has properties similar to those occurring in Range AII, although now a chaotic repeller belonging to the frontier of  $B_\infty$  always exists. The dynamics occurring for  $-1 < b < 0$  have been only partly investigated. We have shown how many attracting cycles may exist, associated (as  $b$  is varied) with fold bifurcations and BCBs, not only of basic cycles with symbolic sequences  $LR^n$  for any  $n \geq 1$  but also of many other infinite families, showing that the bifurcation structure is much richer than that occurring in other systems. In fact, we have seen from the examples in Section 4.1 that the period adding structure is strictly included and the U-sequence cannot be obtained, as flip bifurcations are not allowed. The bifurcation structure strongly depends on the codimension-two points on the BCB curves which we have proved to exist. Moreover, we have shown that BCB curves are limit curves of infinite families of other BCB curves, and that also fold bifurcation and homoclinic bifurcation curves are limit sets of infinite families of BCB curves.

We have numerical evidence (as shown in Figure 1 and in Figure 7) that organizing centres are related to codimension-two points, each one due to intersection of a BCB curve and a fold bifurcation curve of cycles having different symbolic sequences  $LR^n$  and  $LR^{n+1}$ , respectively, occurring at  $a = 0$ . These are issuing points of infinite families of BCB curves and fold bifurcation curves, and left for further investigation.

### Acknowledgements

The first author thanks the Department DESP of the University of Urbino for the hospitality during her stay in Italy. The work of L. Gardini has been done within the activities of the GNFM (National Group of Mathematical Physics, INDAM Italian Research Group), and within the activities of the COST action IS1104 'The EU in the new economic complex geography: models, tools and policy evaluation' [www.gecomplexitycost.eu](http://www.gecomplexitycost.eu).

### Disclosure statement

No potential conflict of interest was reported by the authors.

### Notes

1. Email: [r\\_makrooni@sbu.ac.ir](mailto:r_makrooni@sbu.ac.ir)
2. Email: [f-khellat@sbu.ac.ir](mailto:f-khellat@sbu.ac.ir)

### References

- [1] F. Angulo, M. di Bernardo, E. Fossas, and G. Olivar, *Feedback control of limit cycles: A switching control strategy based on nonsmooth bifurcation theory*, IEEE Trans. Circuits Syst.-I 52(2) (2005), pp. 366–378. doi:10.1109/TCSI.2004.841595.
- [2] V. Avrutin, M. Schanz, and S. Banerjee, *Codimension-three bifurcations: explanation of the complex one-, two-, and three-dimensional bifurcation structures in nonsmooth maps*, Phys. Rev. E 75(6) (2007), p. 066205. doi:10.1103/PhysRevE.75.066205.
- [3] V. Avrutin, P.S. Dutta, M. Schanz, and S. Banerjee, *Influence of a square-root singularity on the behaviour of piecewise smooth maps*, Nonlinearity 23(2) (2010), pp. 445–463. doi:10.1088/0951-7715/23/2/012.

- [4] M. di Bernardo, C.J. Budd, A.R. Champneys, and P. Kowalczyk, *Piecewise-smooth Dynamical Systems: Theory and Applications*, in *Applied Mathematical Sciences*, 163, Springer-Verlag, London, 2008.
- [5] M. di Bernardo, C. Budd, and A. Champneys, *Grazing, skipping and sliding: analysis of the non-smooth dynamics of the DC/DC buck converter*, *Nonlinearity* 11(4) (1998), pp. 859–890. doi:10.1088/0951-7715/11/4/007.
- [6] M. di Bernardo, C.J. Budd, and A.R. Champneys, *Corner collision implies border-collision bifurcation*, *Phys. D* 154(3–4) (2001), pp. 171–194. doi:10.1016/S0167-2789(01)00250-0.
- [7] M. di Bernardo, P. Kowalczyk, and A.B. Nordmark, *Bifurcations of dynamical systems with sliding: derivation of normal-form mappings*, *Phys. D* 170(3–4) (2002), pp. 175–205. doi:10.1016/S0167-2789(02)00547-X.
- [8] L. Gardini, *Homoclinic bifurcations in  $n$ -dimensional endomorphisms, due to expanding periodic points*, *Nonlinear Anal. Theory Methods Appl.* 23(8) (1994), pp. 1039–1089. doi:10.1016/0362-546X(94)90198-8.
- [9] L. Gardini, I. Sushko, V. Avrutin, and M. Schanz, *Critical homoclinic orbits lead to snap-back repellers*, *Chaos Solitons Fract.* 44 (2011), pp. 33–49.
- [10] O. Makarenkov, and S.W. Lamb, *Dynamics and bifurcations of nonsmooth systems: A survey*, *Phys. D* 241(22) (2012), pp. 1826–1844. doi:10.1016/j.physd.2012.08.002.
- [11] R. Makrooni, and L. Gardini, *Bifurcation structures in a family of one-dimensional linear-power discontinuous maps*, *Geocomplexity Discussion Paper N.7* ISSN: 2409-7497. Available at <http://econpapers.repec.org/paper/cstwpaper/> 2015.
- [12] R. Makrooni, N. Abbasi, M. Pourbarat, and L. Gardini, *Robust unbounded chaotic attractors in 1D discontinuous maps*, *Chaos Solitons Fract.* (in press).
- [13] R. Makrooni, F. Khellat, and L. Gardini, *Border collision and fold bifurcations in a family of piecewise smooth maps: Unbounded chaotic sets*, *J. Diff. Equ. Appl.* (in press, 2015).
- [14] R. Makrooni, L. Gardini, and I. Sushko, *Bifurcation structures in a family of 1D discontinuous linear-hyperbolic invertible maps*, Submitted for publication 2015.
- [15] F. Marotto, *Snap-back repellers imply chaos in  $\mathbb{R}^n$* , *J. Math. Anal. Appl.* 63(1) (1978), pp. 199–223. doi:10.1016/0022-247X(78)90115-4.
- [16] F. Marotto, *On redefining a snap-back repeller*, *Chaos Solitons Fract.* 25(1) (2005), pp. 25–28. doi:10.1016/j.chaos.2004.10.003.
- [17] A.B. Nordmark, *Non-periodic motion caused by grazing incidence in an impact oscillator*, *J. Sound Vibr.* 145(2) (1991), pp. 279–297. doi:10.1016/0022-460X(91)90592-8.
- [18] A.B. Nordmark, *Universal limit mapping in grazing bifurcations*, *Phys. Rev. E* 55(1) (1997), pp. 266–270. doi:10.1103/PhysRevE.55.266.
- [19] Z. Qin, J. Yang, S. Banerjee, and G. Jiang, *Border-collision bifurcations in a generalized piecewise linear-power map*, *Discrete Continuous Dyn. Sys. Ser. B* 16(2) (2011), pp. 547–567. doi:10.3934/dcdsb.2011.16.547.
- [20] Z. Qin, Y. Zhao, and J. Yang, *Nonsmooth and smooth bifurcations in a discontinuous piecewise map*, *Int. J. Bifurcation Chaos* 22(5) (2012), 1250112 (7 pages). doi:10.1142/S021812741250112X.